EXPERIMENTAL AND ANALYTICAL STUDIES OF FORMING LIMIT OF AISI 1008 STEEL AND COMPARISON WITH FINITE ELEMENT ANALYSIS

A Major Project Report

Submitted in partial fulfillment of the requirements for the award of degree of

MASTER OF TECHNOLOGY
IN
MECHANICAL ENGINEERING
(CAD/CAM)

By,
Patel Vipul J.
(07MME013)

Department of Mechanical Engineering

INSTITUTE OF TECHNOLOGY

NIRMA UNIVERSITY OF SCIENCE & TECHNOLOGY,

AHMEDABAD 382 481

MAY 2009

Declaration

This is to certify that

i) The thesis comprises my original work towards the degree of Master of Technology in Mechanical Engineering (CAD/CAM) at Nirma University and has not been submitted elsewhere for a degree.

ii) Due acknowledgement has been made in the text to all other material used.

Vipul J Patel

Certificate

This is to certify that the Major Project Report entitled **"Experimental And Analytical Studies of Forming Limit of AISI 1008 Steel and comparison with Finite Element analysis"** submitted by **Mr. Patel Vipul J. (07MME013)**, towards the partial fulfillment of the requirements for the award of Degree of Master of Technology in Mechanical Engineering (CAD/CAM) of Nirma University of_Science and Technology, Ahmedabad is the record of work carried out by him under our supervision and guidance. In our opinion, the submitted work has reached a level required for being accepted for examination. The results embodied in this major project, to the best of our knowledge, have not been submitted to any other University or Institution for award of any degree or diploma.

Prof. V. R. Iyer
Guide, Professor and Head,
Department of Mechanical Engineering,
Institute of Technology,
Nirma University, Ahmedabad.

Mr. Jatin Dave
Co-Guide , Lecturer,
Department of Mechanical Engineering,
Institute of Technology,
NirmaUniversity, Ahmedabad

Mr. Darshan Shah
Guide, Manager,
Design & Engineering,
Harsha Engineers Ltd,
Ahmedabad.

Prof. V. R. Iyer
Professor and Head,
Department of Mechanical Engineering,
Institute of Technology,
Nirma University, Ahmedabad.

Dr. K. Kotecha
Director,
Institute of Technology,
Nirma University,
Ahmedabad.

ACKNOWLEDGEMENT

It is indeed a great pleasure for me to express my gratitude to those who have always helped me throughout my project thesis work.

First of all, I would like to thank my internal project guides ***Prof. V.R.Iyer and Mr.Jatin Dave*** *and* industry guide ***Mr. Darshan Shah*** (Manager, Harsha Engineers Ltd., Changodar) as well as ***Mr. V.P. Mashroo*** (Vice President, HR department, Harsha Engineers Ltd., Changodar) who helped me in pinpointing the need of the project, stimulating suggestions encouragement during all the time of research and also for writing this dissertation. I am sincerely thankful for their valuable guidance and help to enhance my presentation skills.

I would also like to thank ***Mr. Rajubhai Shah*** (M.D., Harsha Engineers Ltd., Changodar) for giving me opportunity to carry out my dissertation at Harsha Engineers Ltd. and for his support and cooperation during my work. my thanks are also due, to H.K.Raval, Professor , Mechanical Engineering, SVNIT, Surat, for providing valuable guidance as and when necessary.

I would also like to thank our course co-ordinator, ***Prof. D.S.Sharma*** for providing valuable guidance and also to the management of Nirma University for providing excellent infrastructure facilities whenever and wherever required.

Finally, I am thankful to all the faculty members of the Mechanical Engineering Department, Laboratory Assistants, Library staff and all my friends and colleagues who have directly or indirectly helped me during this project work.

Vipul J Patel.
07MME013
M.Tech (Mechanical)
(CAD/CAM)

ABSTRACT

The use of sheet metal forming simulations has reduced lead-times and costs for the development of new forming Component significantly. The accuracy of the simulations is to a large extent dependent on the quality of the material properties provided as input to the simulations. Improving the quality of the material properties is the key factor in order to further increase the accuracy of the simulations. So Tensile Test is performed on AISI 1008 steel for determination of Forming Properties of AISI 1008 steel. This study is focused on the forming limit properties of sheet metal. The Purpose of this thesis is to investigate the possibility of replacing time consuming and costly experimental forming limit diagram (FLD) by theoretical and Finite Element Analysis Predicted ones. In this thesis some well-known methods for analytical Prediction of FLD are critically reviewed. The assumptions made in each method are emphasized and their effects on the predicted forming limits are demonstrated. An alternative method, based on Swift's Maximum force criterion, is presented and its merits and demerits are evaluated in comparison with existing methods. Simulations are try out tools for reducing time consuming experimental work. So Finite Element Simulations of Limit Dome Height Test have been performed in order to find the FLD. There are many methods for finding the experimental FLD. In this Experimental work, Limiting Dome Height Test and Erichson test are performed for finding the FLD. Experimental Set up for Limiting Dome Height test is prepared. and find the Forming limit by circle grid analysis method. The accuracy of experimental FLD is large extent dependent on accuracy of circle grid and its measuring system.Finally, Experimental FLD is compared with the theoretical and FEA predicted ones.

LIST OF FIGURES

Chapter 1: Introduction

Fig-1.1 Outline of forming process 3

Fig-1.2 Forming Limit Diagram 4

Chapter 2: Literature Survey

Fig 2.1 Pattern of Grid circle 7

Fig 2.2 Circle Grid 8

Fig 2.3 Pattern of Circular Grid in different Region of FLD 8

Fig 2.4 Mylar Tape 9

Fig 2.5 Effect of dia. of circle grid on FLD 10

Fig 2.6 Effect of specimen direction on FLD 10

Fig 2.7 Effect of thickness on FLD 10

Fig 2.8 Effect of lubrication 11

Fig 2.9 Effect of material on Forming Limit 11

Fig 2.10 Different Zone of Forming Limit Diagram for Aluminum 12

Fig 2.11 Diagram of a perfect strip deformed in uniaxial tension. 13

Fig 2.12. Uniform deformation of part of a continuous sheet in a plane stress Proportional Process 14

Fig 2.13 Comparison of Experimental and theoretical (Hill) FLD 15

Fig 2.14 A local neck formed in a continuous sheet oriented at an angle θ to the maximum principal stress. 16

Fig 2.15. Mohr circle of strain increment to determine the angle of zero extension. 16

Fig 2.16.Geometric M-K Model 17

Fig 2.17.Swift Cup Test 19

Fig 2.18.Erichsen and Olsen test 20

Fig 2.19. Limit Dome Height Test 21

Chapter 3: Evaluation of forming Properties by Uniaxial Tensile Test

Fig 3.1 Experimental Set up for Uniaxial Tensile Test 22

Fig 3.2 Geometry of Test Specimen as per ASTM E8 Standard 23

Fig 3.3 Test Specimen 23

Fig 3.4 Load – Extension Diagram 24
Fig 3.5 Stress Strain Curve 26
Chapter 4 : Theoretical Determination of FLD
Fig 4.1 FLD based on Swift-Hill Model 30
Fig 4.2 FLD based on NADDRG Model 31
Chapter 5: Simulation of Limiting Dome Height test
Fig 5.1 Geometry of LDH Test 32
Fig 5.2 Geometry of Draw bead 32
Fig 5.3 Forming Punch 33
Fig 5.4 Binder 33
Fig 5.5 Die 34
Fig 5.6 Assembly in PRO-E 34
Fig 5.7 Manufacturing Drawing of Forming Punch 35
Fig 5.8 Manufacturing Drawing of Binder 35
Fig 5.9 Manufacturing Drawing of Die 36
Fig 5.10 Assembly of LDH Test 36
Fig 5.11 Workflow Diagram 37
Fig 5.12 Meshing Geometry of LDH Test 38
Fig 5.13 FLD by Hyperform 39
Chapter 6: Experimental determination of FLD by Limiting Dome Height test, Erichson test and tensile test
Fig 6.1 Grid marked on the LDH Test blank 42
Fig 6.2 Experimental Set up for LDH Test 43
Fig 6.3 Tool makers Microscope 43
Fig 6.4 Deformed Specimen of LDH Test 44
Fig 6.5 Forming Limit Diagram based on LDH Test 45
Fig .6.6 Experimental Set Up for Erichson test 46
Fig 6.7 Grid Marked Blank of Erichson Test 47
Fig 6.8 Deformed Specimen of Erichson Test 48
Fig 6.9 Forming Limit Diagram by Erichson Test 49
Fig 6.10 Tensile Test Specimen 49

Fig 6.11 Experimental Set up for Tensile Test 50
Fig 6.12 Deformed Specimen of Tensile Test 50
Fig 6.13-Forming Limit Diagram by Tensile Test 51
Chapter 7: Comparison of FLD by swift-hill model, NADDRG model, Hyperform, Limiting Dome Height test, Erichson test
Fig 7.1 shows Comparison of theoretical FLDs, Experimental FLDs and FE FLD 53

LIST OF TABLES

Table 3.1 Experimental Results from Tensile Test 24
Table 3.2 Results of Calculation 27
Table 3.3 Results of Anisotropy 28
Table 6.1 Bill of Material 40
Table 6.2 Composition of AISI 1008 41
Table 6.3 Blank Dimension of Erichsen Test 47

NOMENCLATURE

w = Width of specimen

t = Thickness of Specimen

l = Length of Specimen

r_0 = Anisotropy in Rolling Direction

r_{45}=Anisotropy in 45° direction

r_{90}=Anisotropy in Longitudinal direction

σ_y= Yield stress of material

σ_u=Ultimate stress of material

n= Strain hardening Exponent

K=Strength Co-efficient

R=Normal Planar Anisotropy Ratio

ΔR = Planar anisotropy coefficient

σ_1=Major Principal Stress

σ_2=Minor Principal Stress

ε_1=Major Strain

ε_2=Minor Strain

$d\varepsilon_1$=Major Strain increment

$d\varepsilon_2$=Minor Strain increment

α = Stress Ratio

β = Strain Ratio

LDH = Limiting Dome Height

FLD = Forming limit Diagram

R00X=Specimen which cut in rolling direction

R45X= Rolled Specimen Which cut in 45 direction

R90X= Rolled Specimen Which cut in 90 direction

AISI = American Iron and Steel Industry

CONTENTS

Certificate

Acknowledgement

Abstract

List of Figure/Tables

Chapter 1: Introduction 1

1.1 Sheet metal forming operations 2

1.2 Important Characteristics in Sheet Forming 2

1.3 Outline of Forming Process 3

1.4 Forming Limit Diagram 4

Chapter 2: Literature Survey 6

2.1 Anisotropy 6

2.2 Circle Grid Method 7

2.2.1 Grid 7

2.2.2 Strain Measurement 9

2.3 Factors affecting the zone of critical deformation 9

2.3.1 Diameter of the circular grid 10

2.3.2 Direction of specimen with respect to rolling 10

2.3.3 Thickness of the sheet 10

2.3.4 Effect of Lubrication 11

2.4 Effect of Material on Forming Limit 11

2.5 Theoretical Model of FLD 12

2.5.1 Swift's Maximum Force Criterion For Diffuse Neck (Considering Uni-Axial Tension) 12

2.5.2 Hill Criterion for localized Necking 14

2.5.3 Comparision of Experimental and theoretical (Hill) FLD 15

2.5.4 Marciniak-Kuczinski Model for FLD Prediction 17

2.6 Formability Testing Methods 18

2.6.1 The Swift cup test 18

2.6.2 Erichsen and Olsen tests 20

2.6.3 Limiting Dome Test 20
Chapter 3: Evaluation of forming Properties by Uniaxial Tensile Test 22
3.1 Uniaxial Tensile Test 22
3.1.1 Experimental Procedure 22
3.1.2 Theoretical calculation of R003 Specimen 24
Chapter 4 : Theoretical Determination of FLD 29
4.1 Swift-Hill Model 29
4.2 NADDRG Model 31
Chapter 5: Simulation of Limiting Dome Height test 32
5.1 Modeling of LDH Test 32
5.1.1 Procedure of Modeling 32
5.2 Analysis of LDH Test 36
Chapter 6: Experimental determination of FLD by Limiting Dome Height test, Erichson test and tensile test 40
6.1 Limiting Dome Height Test 40
6.1.1 Press Specification 40
6.1.2 Blank Specification 41
6.1.3 Chemical Analysis of Blank 41
6.1.4 Circle Grid Marking 42
6.1.5 Experimental Set up 43
6.1.6 Grid Measurement System 43
6.1.7 Experimental Procedure for Determination of FLD 44
6.1.8 Results from LDH Test 44
6.2 Erichsen Test 46
6.2.1 Specification of Erichson Testing Machine 46
6.2.2 Circle Grid Marking 47
6.2.3 Blank Specification 47
6.2.4 Experimental Procedure 47
6.2.5 Experimental FLD by Erichson Test 48
6.3 Tensile Test 49
6.3.1 Specimen Used for Experimental Work 49

6.3.2 Circle Grid Marking 50
6.3.3 Experimental Procedure 50
6.3.4 Forming Limit Diagram by Tensile Test 51
Chapter 7: Comparison of FLD by swift-hill model, NADDRG model, Hyperform, Limiting Dome Height test, Erichsen test 53
Chapter 8 : Conclusion & Future Scope 54
References 56

CHAPTER-1 INTRODUCTION

Modern continuous rolling mills produce large quantities of thin sheet metal at low cost. A substantial fraction of all metals are produced as thin hot-rolled strip or cold-rolled strip. This is then formed in secondary processes into automobiles, domestic appliances, building products, aircraft, food and drink cans and a host of other familiar products. Sheet metals parts have the advantage that the material has a high elastic modulus and high yield strength so that the parts produced can be stiff and have a good strength-to-weight ratio.

Sheet metal forming technology is therefore an important engineering discipline within the area of mechanical engineering. Sheet metals are characterized by a high ratio of surface area to thickness. Sheet metal forming is basically conversion of a flat sheet metal into a product of desired shape without defect like fracture or excessive localized thinning.

In automobiles the sheet metal is deformed into the desired and brought into the required form to get autobody pressings like bonnet, bumpers, doors, etc. In aircraft's sheet metal is used for making the entire fuselage wings and body. In domestic applications sheet metal is used for making many parts like washing machine body and covers, iron tops, timepiece cases, fan blades and casing etc. The products made by sheet-forming processes include a large variety of shapes and sizes, ranging from simple bends to double curvatures with shallow or deep recesses. Typical examples are metal desks, appliance bodies, aircraft panels, beverage cans, auto bodies etc.

The industrial process of sheet-metal forming is strongly dependent on numerous interactive variables: material behavior, lubrication, forming equipment etc. One of the main limitations in industrial stampings seems to be the appearance of localized necking. The material ability to deform plastically depends on a great number of interactive parameters whose experimental study is a difficult task. The theoretical analysis of plastic instability is therefore of major importance in order to predict the forming limit strains, examine the influence of each parameter on the necking occurrence and improve the press performance. The forming limit diagram represents a useful concept on sheet-metal formability characterization and a very important safety tool in sheet-metal forming simulation.

Traditional evaluation of formability is based on both intrinsic tests and simulative tests. The intrinsic tests measure the basic characteristic properties of materials that can be related to their formability. These tests provide comprehensive information that is insensitive to the thickness

and surface condition of the material. Examples of intrinsic tests are Uniaxial tensile test, Plane strain tensile test, Marciniak Biaxial Stretching test, Hydraulic Bulge test, Marciniak In-Plane Sheet torsion test, Miyauchi shear test, Hardness test. The simulative tests subject the material to deformation that closely resembles the deformation that occurs in a particular forming operation. Examples of these tests include Erichsen, Olsen, Fukui, Swift tests.

1.1 Sheet metal forming operations

- The amount of useful deformation is limited by the occurrence of unstable deformation which mainly takes the form of localized necking or wrinkling.
- Failure by wrinkling occurs when the dominant stresses are compressive, tending to cause thickening of the material.
- Localized necking occurs when the stress state leads to an increase in the surface area of the sheet at the cost of a reduction in the thickness.

There are two kinds of neck :-

- The diffuse neck (extension is much greater than the sheet thickness)
- Localized necking (through thickness thinning) Terminated by final separation or fracture.

Localized neck is a very important phenomenon in determining the amount of useful deformation that can be imposed on a work piece.

The mechanism for the initiation of the localized band is very complicated, roughly speaking, this phenomenon can be attributed to the softening effect.

1.2 Important Characteristics in Sheet Forming

- **Elongation:** Determines the capability of the sheet metal to stretch without necking and failure; high strain-hardening exponent (n) and strain-rate sensitivity exponent (m) desirable.
- **Anisotropy (planar):** Exhibits different behavior in different planar directions present in cold-rolled sheets because of preferred orientation or mechanical fibering, causes earing in drawing, can be reduced or eliminated by annealing but at lowered strength.
- **Anisotropy (normal):** Determines thinning behavior of sheet metals during stretching important in deep-drawing operations.

- **Grain size:** Determines surface roughness on stretched sheet metal; the coarser the grain, the rougher the appearance (orange peel); also affects material strength.
- **Residual stresses :** Caused by non uniform deformation during forming causes part distortion when sectioned and can lead to stress-corrosion cracking; reduced or eliminated by stress relieving.
- **Spring back:** Caused by elastic recovery of the plastically deformed sheet after unloading causes distortion of part and loss of dimensional accuracy can be controlled by techniques such as over bending and bottoming of the punch.
- **Wrinkling:** Caused by compressive stresses in the plane of the sheet can be objectionable or can be useful in imparting stiffness to parts can be controlled by proper tool and die design.
- **Surface condition of sheet:** Depends on rolling practice important in sheet forming as it can cause tearing and poor surface quality.

1.3 Outline of Forming Process

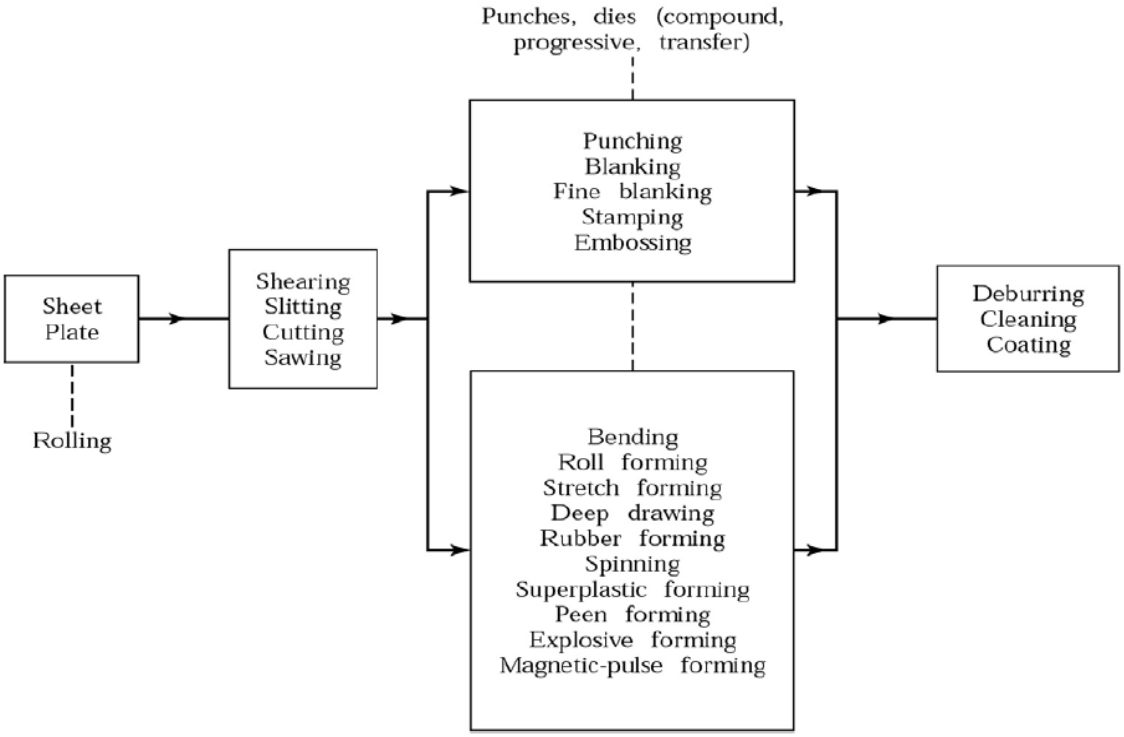

Fig 1.1 Outline of forming Process

1.4 Forming Limit Diagram

The forming limit diagram shows the localization (called forming limit) and failure strains by relating the maximum (major) to minimum (minor) Strain in two dimensional strain space.

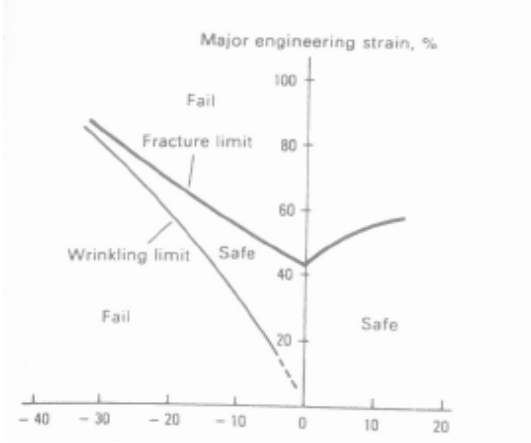

Minor Engineering Strain(%)

Fig-1.2 Forming Limit Diagram

After the introduction of the Forming Limit Diagram (FLD)s concept by Keeler and Backofen and Goodwin, the research in this field of sheet-metal formability has focused mainly on the development of some mathematical models for theoretical determination of FLDs. Hill is the first who proposed a general criterion for localized necking in thin sheets under plane stress states. His analysis predicts localized plastic deformation in the negative minor strain region. Marciniak and Kuckzinsky (M–K) have proposed the first realistic mathematical model for theoretical determination of FLDs that suppose an infinite sheet metal containing a region of local imperfection where heterogeneous plastic flow develops and localizes. Hutchinson and Neale extended M–K theory using a J2 deformation theory. Therefore, the left and right hand sides of the forming limit diagram can be calculated by M–K analysis. The bifurcation theory represents another approach of sheet necking description (valid for homogeneous materials) that predicts the entire FLD for linear strain paths. A general result is that the predicted limit strains tend to strongly depend on the constitutive law incorporated in the analysis. The use of an appropriate yield function that describes analytically the plastic behavior of orthotropic metals allows to a better prediction of limit strains, therefore a better shape and position of FLDs.

Instability predictions are important in sheet-metal forming processes, one such instability being splitting failures due to localized necking. The majority of such sheet-metal industrial splitting

failures occur near to the plane-strain state. Therefore, sheet-metal industries have always been looking for an "ideal" formability test which allows them to evaluate sheets for their ability to resist splitting failures under near plane-strain conditions. Several formability tests have been developed in the past but none have been very successful. But today Limiting Dome test (LDH) test is considered best formability test for industry because it is fast and easy to perform, results are Reproducible and Cost Effective.

CHAPTER-2 LITERATURE SURVEY

2.1 Anisotropy [3]

Material in which the same properties are measured in any direction is termed isotropic, but most industrial sheet will show a difference in properties measured in test-pieces aligned, for example, with the rolling, transverse and 45◦ directions of the coil. This variation is known as planar anisotropy. In addition, there can be a difference between the average of properties in the plane of the sheet and those in the through-thickness direction. In tensile tests of a material in which the properties are the same in all directions, one would expect, by symmetry, that the width and thickness strains would be equal; if they are different, this suggests that some anisotropy exists.

In materials in which the properties depend on direction, the state of anisotropy is usually indicated by the *R-value*. This is defined as the ratio of width strain, $\varepsilon_w = \ln(w/w_0)$, to thickness strain, $\varepsilon_t = \ln(t/t_0)$. In some cases, the thickness strain is measured directly, but it may be calculated also from the length and width measurements using the constant volume assumption, i.e.

$$wtl = w_0 t_0 l_0$$

or

$$\frac{t}{t_0} = \frac{w_0 l_0}{wl}$$

The *r*-value is therefore,

$$r = \frac{\ln \frac{w}{w_0}}{\ln \frac{w_0 l_0}{wl}}$$

If the change in width is measured during the test, the R-value can be determined continuously and some variation with strain may be observed. Often measurements are taken at a particular value of strain, e.g. at $e_{eng.} = 15\%$. The direction in which the R-value is measured is indicated by a suffix, i.e. r_0, r_{45} and r_{90} for tests in the rolling, diagonal and transverse directions respectively. If, for a given material, these values are different, the sheet is said to display planar anisotropy and the most common description of this is

$$\Delta R = \frac{r_0 + r_{90} - 2r_{45}}{2}$$

which may be positive or negative, although in steels it is usually positive.

If the measured R-value differs from unity, this shows a difference between average in-plane and through-thickness properties which is usually characterized by the normal plastic anisotropy ratio, defined as

$$R = \frac{r_0 + 2r_{45} + r_{90}}{4}$$

2.2 Circle Grid Method [7]

Strain analysis by grid marking is a useful method, which has been used effectively to solve the problems in metal forming. When sheet metal is formed, its surface is subjected to different stresses. This results into non uniform strains to be developed in the formed part. Thus there will be regions of high strains as well as low strains, which may lead to wrinkling or fracturing of the material. By the grid marking method the areas of high strain can be easily identified. The sheet is marked with the grid before forming process is carried out. After the sheet metal is deformed into desired shape, strain distribution can be visualized and critical areas of strain will be found by FLD (forming limit diagram) and control can be planned by varying the forming parameters.

2.2.1 Grid [7, 16]

Many types of circle grid patterns have been used, such as square arrays of contacting or closely spaced non contacting circles and arrays of overlapping circles. With small closely spaced circles, it is possible to determine strain gradients accurately. After deformation the circle is transferred into ellipse. The direction of the strains is indicated by the major and minor axis of the ellipse. Circles of 2.5mm diameters have been found to be a good size.

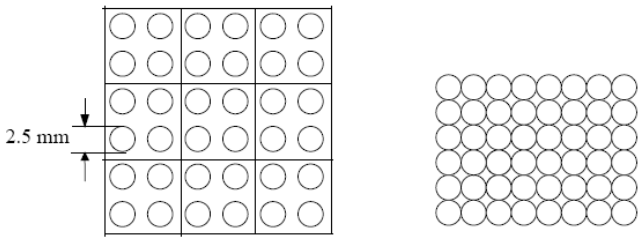

Fig 2.1 Patterns of Circle Grids

After sheet metal is formed the marked circles will deform into ellipses of different sizes. Strain is calculated from the following formula

Taking,

Major strain $\varepsilon_1 = \frac{(L_1 - d)}{d} * 100$ (a)

Minor strain $\varepsilon_2 = \frac{(L_2 - d)}{d} * 100$ (b)

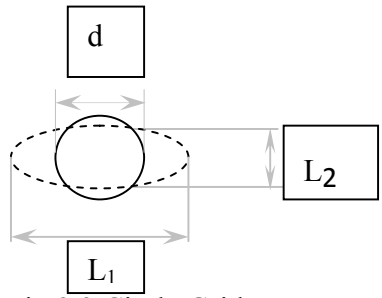

Fig 2.2 Circle Grid

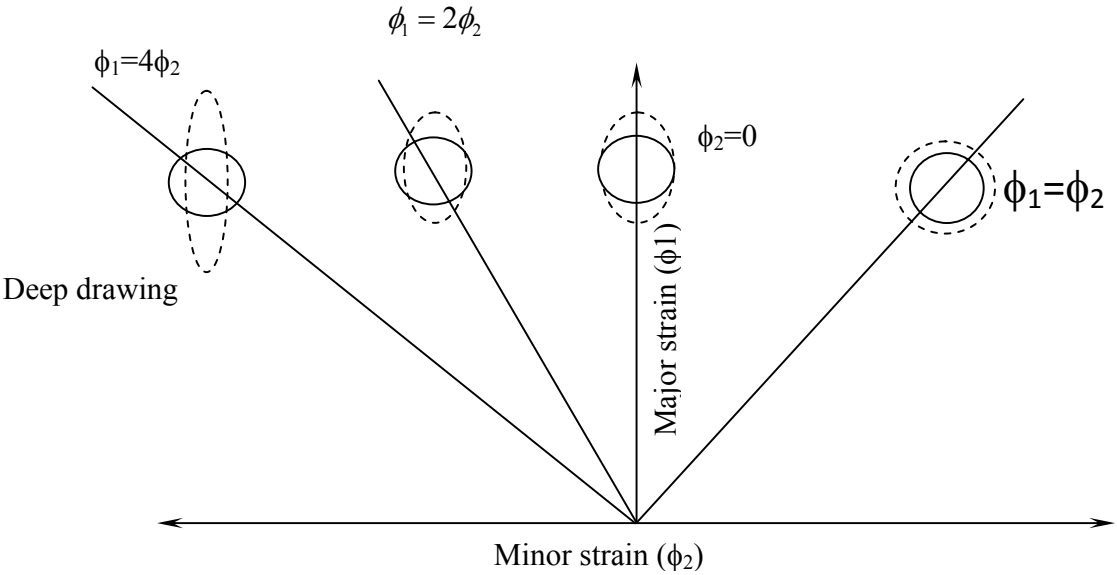

Fig 2.3 Pattern of Circular Grid in different Region of FLD

The circular pattern etched will deform differently according to the type of loading. In this plot, there is relationship between the distortion of the circle and the type of stressing. The maximum strain will be along the major axis and the minimum strain will be perpendicular to major axis i.e., along the minor axis. The strain plots are at the critical points where cracks are likely to form. There is a zone of critical deformation between the good and failure zone. The zone between these boundaries denotes areas of instability.

2.2.2 Strain Measurement[17]

1) **Dividers and steel rule** - This is the most simple and quick method. This method is suitable for measurement on more or less flat surface. On curved surface the measured dimension will be less i.e. it will measure the chord length rather than arc length. The accuracy is also limited.

2) **Mylar Tape** – this is a transparent scale to measure the strain directly. This tape has diverging lines scaled to read directly in percent strain. This scale is produced by photographic printing from a negative on to film. The scale is placed over an ellipse over a sharp radius and then shifted until the diverging lines line up with the major axis of the ellipse. The percent strain is measured directly from the scale. The scale is next turned 90 degrees to read the minor strain.

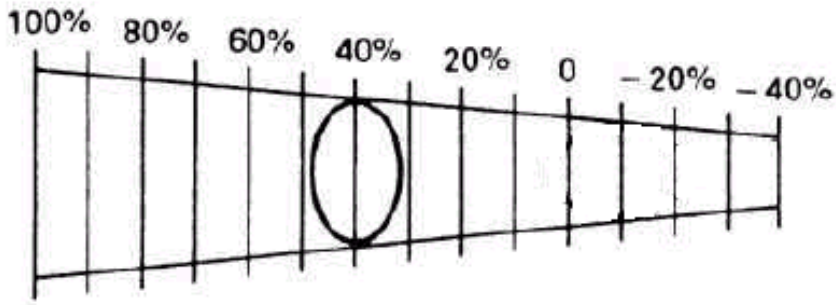

Fig 2.4 Mylar Tape

3) **Travelling microscope** - This is the most widely used method for measuring the changes in the dimension of grid circles. There are two right angle slides on which work is mounted. The work is positioned under the microscope. Cross wire is aligned at one end and the measurement is taken. The cross wire is then aligned on the other end by moving the work table and the measurement is taken. The difference between the two readings gives the absolute measurement. This is an accurate method. Two persons can get different readings because of error in aligning the two axes.

2.3 Factors affecting the zone of critical deformation [7]

2.3.1 Diameter of the circular grid

Area of the safe zone increases with reduction in diameter of the etched circular grid as shown in Fig.2.5. So it is desirable to have smallest possible diameter in etching during testing

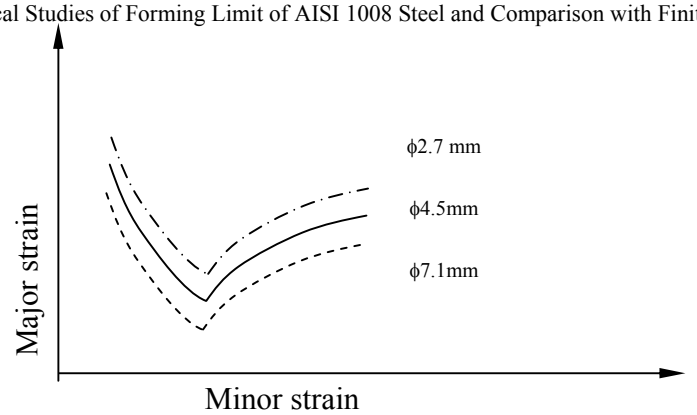

Fig 2.5 Effect of dia. of circle grid on FLD

2.3.2 Direction of specimen with respect to rolling

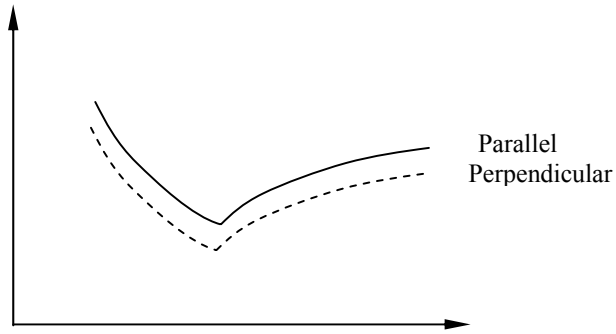

Fig 2.6 Effect of specimen direction on FLD

If the elongation is along the direction of rolling the safe zone will be more comparing the other (elongation perpendicular to direction of rolling) while all other parameters kept constant.

2.3.3 Thickness of the sheet

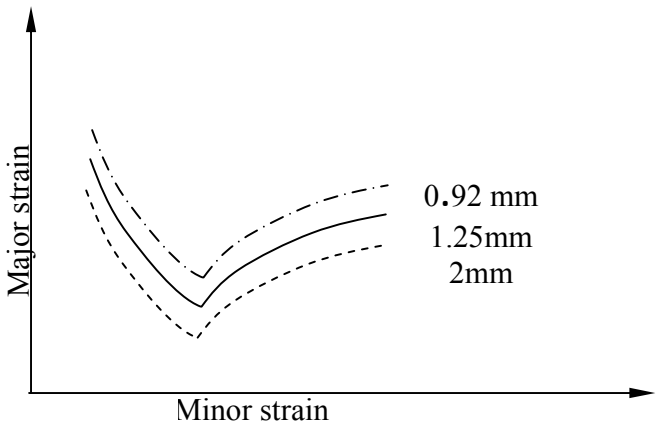

Fig 2.7 Effect of thickness on FLD

For lesser thickness, area of safe zone is more than that of greater thickness as shown in Fig2.7.

2.3.4 Effect of Lubrication

For better lubrication the area of safe zone is increased than the poorer lubrication

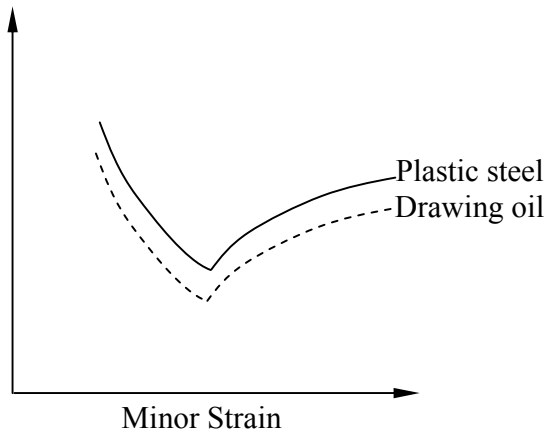

Fig 2.8 Effect of lubrication

2.4 Effect of Material on Forming Limit

Different material have different properties so they have different forming limit which can be understand by Figure 2.9

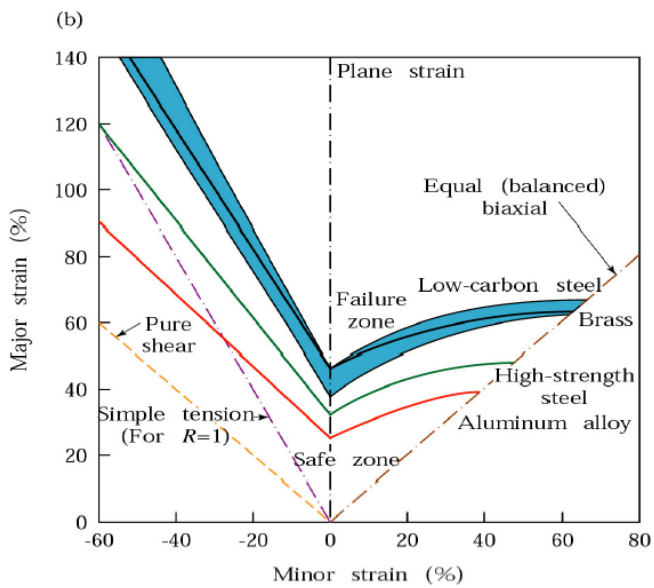

Fig 2.9 Effect of material on Forming Limit

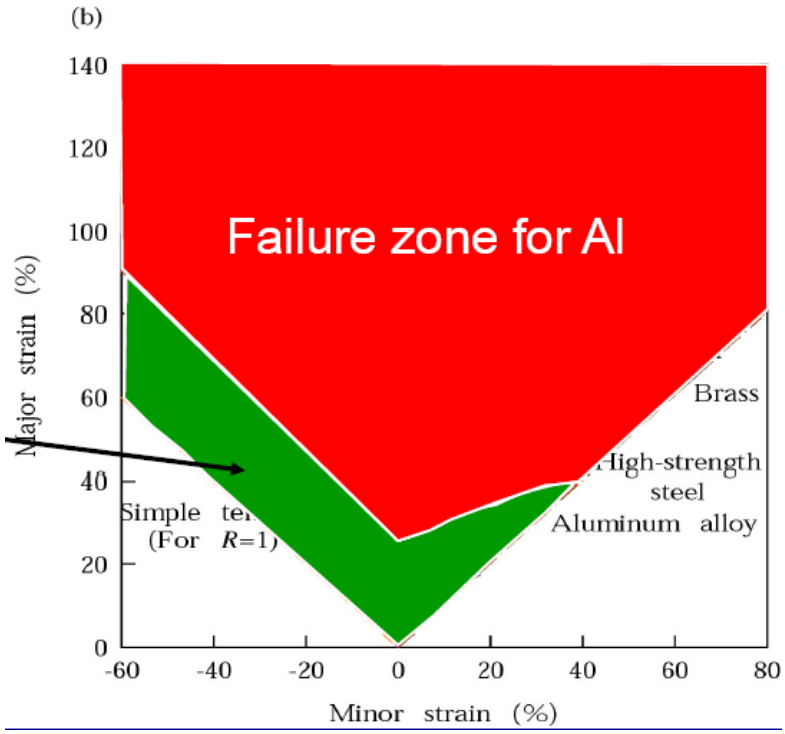

Fig 2.10 Different Zone of Forming Limit Diagram for Aluminum

2.5 Theoretical Model of FLD

2.5.1 Swift's Maximum Force Criterion For Diffuse Neck(Considering Uni-Axial Tension)[1]

In Swift Criterion first consider the theoretical case of a parallel strip of metal, as in the gauge length of a tensile test-piece. Swift consider that the properties are uniform throughout and the geometry is perfect. When this is stretched in tension as shown in Figure 2.1, the volume remains constant and the following relations apply. The cross-sectional area is A = wt and the volume is

$$Al = A_0 l_0 \tag{1}$$

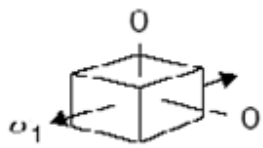

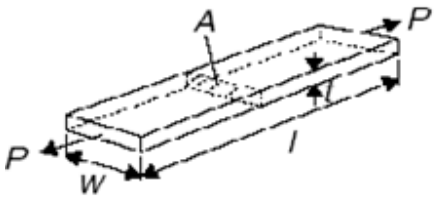

Fig 2.11 Diagram of a perfect strip deformed in uniaxial tension.

Differentiating Equation 1, We Obtain

$$\frac{dA}{A}+\frac{dl}{l}=0 \qquad \text{or} \qquad \frac{dl}{l}=d\varepsilon_1=-\frac{dA}{A} \tag{2}$$

The Strain in the Strip is

$$\varepsilon_1 = \ln\frac{l}{l_0} \tag{3}$$

And Stress is,

$$\sigma_1=\frac{P}{A}=\frac{P}{A_0}\frac{l}{l_0} \tag{4}$$

The load in the strip is P = σ_1A; as the strip deforms, σ1 will increase for a strain hardening material and the cross-sectional area will decrease, i.e. dσ_1 will always be positive and dA will be negative. At some stage, the rate of strain-hardening will fall below the rate of reduction in area and the load will reach a maximum. At this instant,

$$dp=d(\sigma_1 A)=0 \tag{5}$$

$$\frac{dp}{p}=\frac{d\sigma_1}{\sigma_1}+\frac{dA}{A}=0 \tag{6}$$

$$\frac{1}{\sigma_1}\frac{d\sigma_1}{d\varepsilon_1}=1 \tag{7}$$

The function on the left-hand side of Equation 7 is a material property that is known as the non-dimensional strain-hardening characteristic and it could be determined from a material test. If the material obeys a simple power law, $\sigma_1 = K\varepsilon^n{}_1$ this function is

$$\frac{1}{\sigma_1}\frac{d\sigma_1}{d\varepsilon_1}=\frac{nK}{\sigma_1}(\varepsilon_1)^{n-1}=\frac{n}{\varepsilon_1} \tag{8}$$

Combining Equations 7 and 8,

$$\frac{1}{\sigma_1}\frac{d\sigma_1}{\sigma_1} = \frac{n}{\varepsilon_1} = 1$$

And the Strain at the maximum load is

$$\varepsilon_1^* = n \tag{10}$$

2.5.2 Hill Criterion for localized Necking [2]

In Hill Criterion, consider a region of the sheet deforming uniformly in a proportional process as shown in Figure 2.2. The deformation in this region may be specified as

$$\sigma_1; \quad \sigma_2 = \alpha\sigma_1; \; \sigma_3 = 0$$
$$\varepsilon_1; \; \varepsilon_2 = \beta\varepsilon_1; \; \varepsilon_3 = -(1+\beta)\varepsilon_1 \tag{11}$$

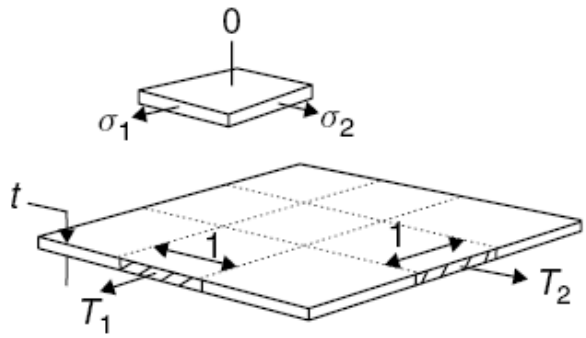

Fig 2.12. Uniform deformation of part of a continuous sheet in a plane stress proportional process

The principal tensions in the sheet are

$$T_1 = \sigma_1 t \;\text{ and }\; T_2 = \alpha T_1 = \sigma_2 t \tag{12}$$

The condition postulated for local necking is that it will start when the major tension reaches a maximum. As the process is proportional, α and β will be constant. Differentiating Equation 12, we obtain

$$\frac{dT_1}{T_1} = \frac{d\sigma_1}{\sigma_1} + \frac{dt}{t} = \frac{d\sigma_1}{\sigma_1} + d\varepsilon_3 = \frac{d\sigma_1}{\sigma_1} - (1+\beta)d\varepsilon_1 \tag{13}$$

When the tensions reach a maximum, Equation 13 becomes zero and the non-dimensional strain-hardening is,

$$\frac{1}{\sigma_1}\frac{d\sigma_1}{d\varepsilon_1} = 1+\beta \tag{14}$$

Differentiating generalized Stress-strain law, $\sigma_1 = K'\varepsilon_1^n$,

$$\frac{1}{\sigma_1}\frac{d\sigma_1}{d\varepsilon_1} = \frac{n}{\varepsilon_1} \tag{15}$$

Substituting Eq.15 in Eq.14, we get,

$$\varepsilon_1^* = \frac{n}{1+\beta} \text{ and } \varepsilon_2^* = \frac{\beta n}{1+\beta} \tag{16}$$

$$\varepsilon_1^* + \varepsilon_2^* = n$$

Where Star indicates the Strain at maximum Tension.

2.5.3 Comparison of Experimental and theoretical (Hill) FLD [3]

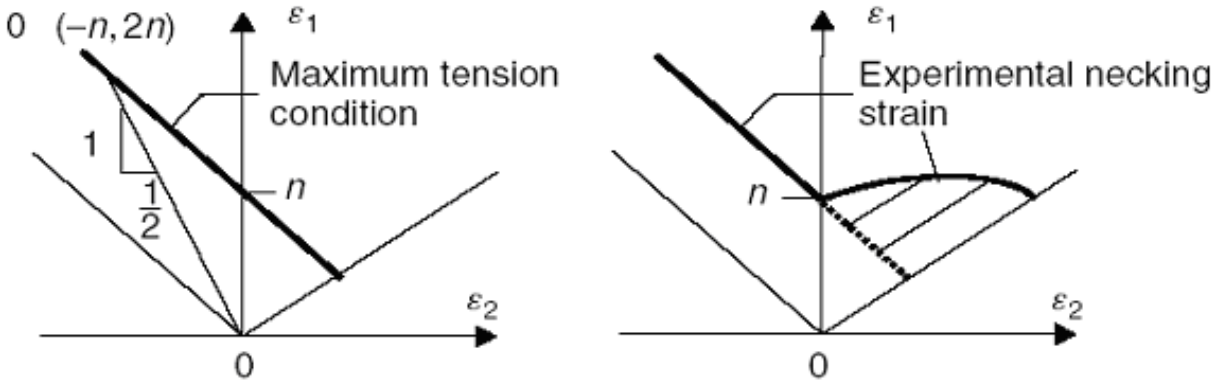

Fig 2.13 Comparison of Experimental and theoretical (Hill) FLD

Why Hill Criterion Fails to predict forming limit in right hand side of FLD

- ❖ Assumption Of Hill Theory
- ➢ The stress and strain ratios must remain constant, as assumed in the differentiation, both before and during the necking process.
- ➢ For the process to be a local one, the necking process should not affect the boundary conditions in Figure 2.11

The second condition ensures that the neck must take the form of a narrow trough in the sheet, as in Fig 2.14, rather than as a patch or diffuse region that would influence conditions away from the neck.

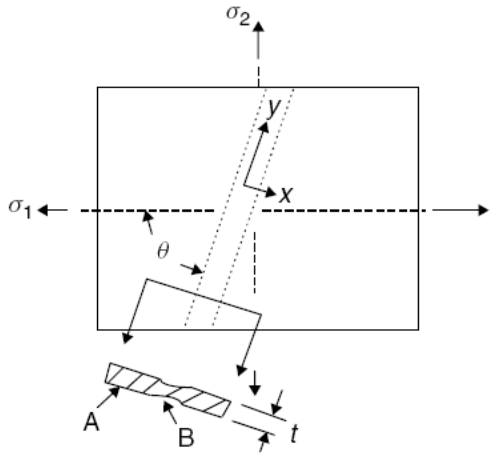

Figure 2.14 A local neck formed in a continuous sheet oriented at an angle θ to the maximum principal stress.

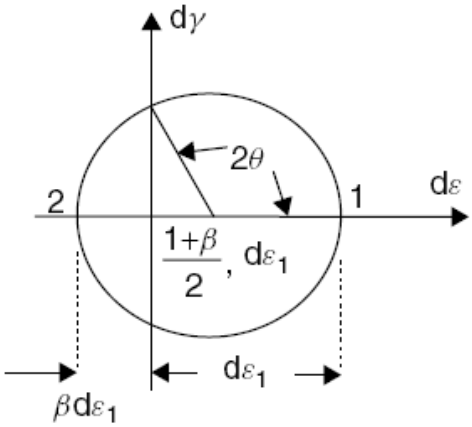

Figure 2.15. Mohr circle of strain increment to determine the angle of zero extension.

Once the necking process becomes catastrophic, in the sense that the uniform region A ceases to strain, the strain increment parallel to the neck, in the y direction in Figure 2.14, will be zero. Geometric constraint requires that the strain increment along the neck must be equal to that in the same direction just outside it; i.e. the strain increment in the y direction in both regions A and B along the neck, must be zero. The first condition above requires that the strain ratio does not change, the second that it is zero during necking, therefore the strain increment in the y direction must be zero at all times, i.e. the neck can develop only along a direction of zero extension. This direction of the neck can be found from the Mohr circle of strain increment shown in Figure 2.15.

The centre of the circle is at

$$\frac{1+\beta}{2} d\varepsilon_1$$

And the radius of the circle is

$$\frac{1-\beta}{2} d\varepsilon_1$$

The direction of zero extension, $d\varepsilon_y = 0$, is given by

$$\cos 2\theta = \frac{1+\beta}{1-\beta}$$

If $\beta > 0$, there is no direction in which the extension is zero. So hill Criterion fails in the negative strain space.

2.5.4 Marciniak-Kuczinski Model for FLD Prediction [4]

The M-K model assumes that the strain localization appears in the region of a material or geometrical inhomogeneity. The initial groove or trough is assumed to develop when proportional loading is applied outside the groove.

The force equilibrium ensures that the strain level within the groove grows faster than the strain outside, until eventually a plane strain condition is reached with in the groove. At this point, the material is assumed to lose its capability for carrying additional load, and localized necking occurs. The M-K method has been used widely in predicting forming limits of sheet metals.

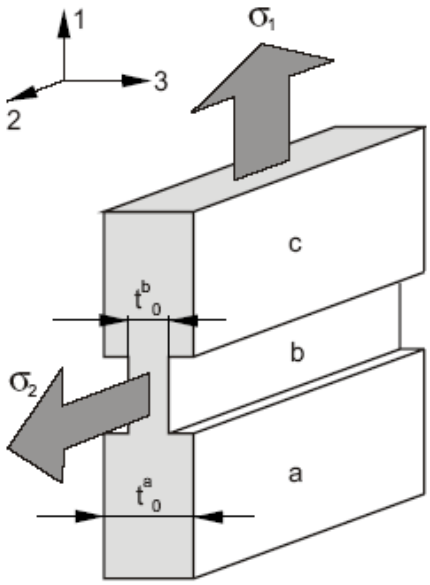

Fig 2.16.Geometric M-K Model

The model presented assumes the existence of a geometric non-homogeneity in the form of notch perpendicular to the direction of the maximum principal stress σ_1.The initial thickness of the

sheet metal t^a_0 is greater than the initial thickness in the region which contains an imperfection t^b_0.The sheet metal is stretched the principal stresses σ_1 and σ_2. The Current value of the inhomogeneity coefficient is expressed by the relationship.

$$f_0 = \frac{t_b}{t_a}$$

Where t_a and t_b are the current values of the thickness in the regions a and b respectively.

For each of the two regions of the sheet are valid the following levy-Mises equations and Hollomon's equation respectively.

The model is completed with two equations the link between regions a and b.Equation expressing the equilibrium of the interface of the two regions.

$$\sigma_{1a}.t_a = \sigma_{1b}.t_b$$

Equations expressing the fact that the strains parallel to the notch are equal in both regions.

$$d\varepsilon_{2a} = d\varepsilon_{2b}$$

2.6 Formability Testing Methods

The important modes of deformation that can exist in a industrial stamping are drawing and stretching. Several formability tests have been developed that simulate drawing and or stretching conditions existing in press-forming operations: such formability tests are termed "Simulative Tests".

Some of the popular simulative tests are:

1. The Swift cup test
2. The Erichsen and the Olsen dome tests
3. The LDH test

2.6.1 The Swift cup test [5,6]

The Swift cup test simulates drawing operations and thus evaluates the sheet metal's drawability. The test involves drawing a small flat-bottomed parallel-sided

cup, in which the sheet is held under a blank-holder, but is welt lubricated to ensure that it can be drawn under the blank-holder.

The drawability of the sheet metal is estimated by drawing series of blanks of increasing diameter. The maximum blank size that can be drawn without fracture occurring over the punch nose is used to calculate the limiting draw ratio (LDR):

LDR = maximum blank diameter/cup diameter.

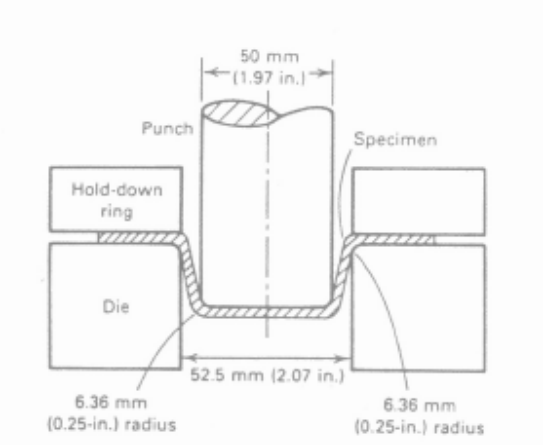

Figure 2.17.Swift Cup Test

The Swift cup test is well suited to predict the performance of sheet metals in deep-drawn components. This test is time consuming and is not suited for predicting
Sheet-metal behavior in stamping that involve stretching operations.

2.6.2 Erichsen and Olsen tests[5,6]

The Erichsen and the Olsen tests were the first tests developed to estimate sheet metal formability under stretching conditions. In both tests, the sheet is clamped between two polished fiat plates with a hole of diameter equal to 25.4 mm and a ball of diameter, d, is pressed into the sheet metal until failure occurs. The height of the cup, h, at failure is used as the formability index (d for Olsen test is equal to 22.2 mm and for Erichsen test d is equal to 20 mm). The larger this height, h, the greater is the sheet metals ability to resist necking instability during stamping.

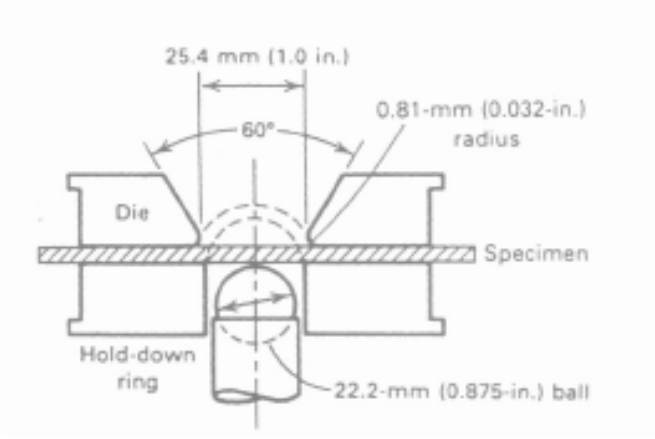

Figure 2.18.Erichsen and Olsen test

The Erichsen and the Olsen tests are no longer favored because of poor reproducibility of data and lack of correlation with either other mechanical properties or service experience. Hecker attributes this to insufficient size of the penetrator, the inability to prevent inadvertent drawing in of the flange and inconsistent lubrication. Hecker noted that bending strains are normally minimal during the stamping of a large sheet, whereas the small punch used in the Erichsen/ Olsen test produces significant bending strains in the sheet; moreover, Hecker remarked that the clamping plates were not effective in keeping the sheet from drawing into the die cavity. The amount of draw-in was not identical from test to test and thus was seen as a great source of the variability in the data.

2.6.3 Limiting Dome Test[5,6,7]

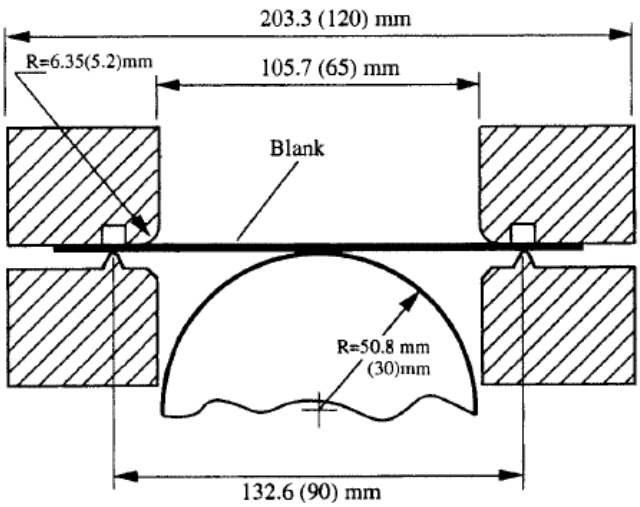

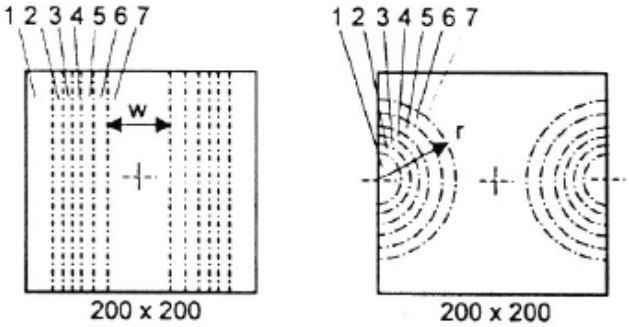

Specimen	1	2	3	4	5	6	7
w	200	120	100	85	70	55	40
r	0	40	50	57.5	65	72.5	80

Figure 2.19. Limit Dome Height Test[14]

The LDH test is developed to simulate more effectively the fracture conditions
(plane strain) found in most stampings. In this test a 102 mm diameter hemispherical punch is used and sheet-metal strips of varying width are clamped rigidly in a blankholder and then stretched over the punch. The metal strips are marked with a grid of small circles (2.5 mm diameter) and the width strain at the fracture site is measured from the circle closest to the fracture. This width strain is minimum (close to plane strain) at some critical blank width of the sheet metal. Correspondingly, the height at which the dome fails shows a minimum at the critical blank-width. This minimum height is known as the limiting dome-height near plane strain (LDHo) and is used extensively as a formability index. LDH results correlate well with the total elongation observed in a tensile test. The LDH test results also correlate well with the stamping behavior.

As the LDH test is able to simulate the most critical strain state observed in stamping (plane-strain conditions), it is the most popular test used in industry.

CHAPTER-3 EVALUATION OF FORMING PROPERTIES BY TENSILE TEST

3.1 Uniaxial Tensile Test[8]

In currently engineering world, Lead Time for the Development of new forming component is very crucial. Each and Every industry uses a Sheet Metal Forming Simulation software for reducing Lead Time for the Development of new forming component. The accuracy of the simulations is to a large extent dependent on the quality of the material properties provided as input to simulations. A material property is the key factor in order to further increase the accuracy of simulation. So Tensile Test is performed for AISI 1008 on universal tensile testing machine and determines the Mechanical Properties.

3.1.1 Experimental Procedure:

Tensile testing machine is built up with a load frame of a solid T-slot table, columns and a hydraulically maneuverable crosshead. Control and data acquisition is performed by computer boards and specially designed programs. Test is performed on Universal Tensile Testing machine which is manufactured by FIE. To be able to clamp the specimen in the desirable manner, special attention was put on the rectangular jaw rather than circular jaw, and specially their surface towards the specimen.

Fig 3.1 Experimental Set up for Uniaxial Tensile Test

After completing the Tensile Test we have get the output in graph manner which are load – extension diagram and stress – strain curve with yielding load, Ultimate Tensile Load and Final gauge length of the Tensile Test Piece.

The geometry of the test Specimen is as per ASTM Standard Which are shown in the figure. The Specimen cut on the Wire Cutting Machine.

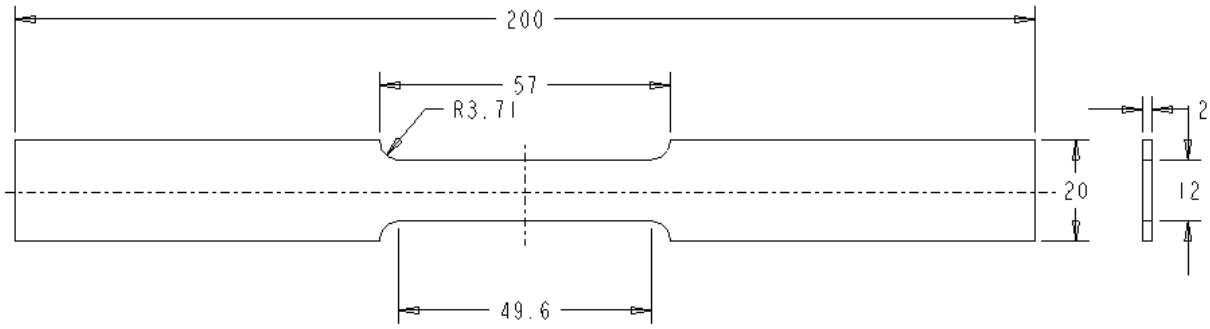

Fig 3.2 Geometry of Test Specimen as per ASTM E8 Standard

Fig 3.3 Test Specimen

Total Nine Tensile Test Specimens

- ✓ Three for Rolling Specimen which cut in coil winding direction (r_0).
- ✓ Three for Angular Specimen which cut in 45° direction (r_{45}).
- ✓ Three for Transverse Specimen which cut in 90° direction (r_{90}) are used to find the value of r_0, r_{45}, r_{90}.

DATA FROM TENSILE TEST:

Specimen Type	Final Gauge Length	Final width	Final Thickness	Ultimate Load	Yield Load	Disp.at Max.load	Max. Disp.	Ultimate Stress (Eng.)	Yield Load
R001	72.80	8.7	1.633	7790	255	19.00	22.80	311.600	6375
R002	71.90	9.260	1.591	8190	275	14.30	21.90	327.600	6875
R003	71.90	9.280	1.531	7960	250	12.80	21.90	318.400	6250
R451	71.40	9.050	1.650	7700	270	13.20	21.40	308.00	6750
R452	73.50	8.560	1.631	7830	252	13.30	23.50	313.200	6312
R453	72.00	9.220	1.642	8000	267.50	13.90	22.00	320.00	6687

R901	69.60	9.510	1.642	7660	252.50	13.10	19.60	306.400	6312
R902	70.40	8.310	1.628	8050	270	13.00	20.40	322.00	6750
R903	69.90	9.130	1.652	7850	250	12.90	19.90	314.00	6250

Table 3.1 Experimental Results from Tensile Test

3.2 Theoretical Calculation for R003 Specimen:-

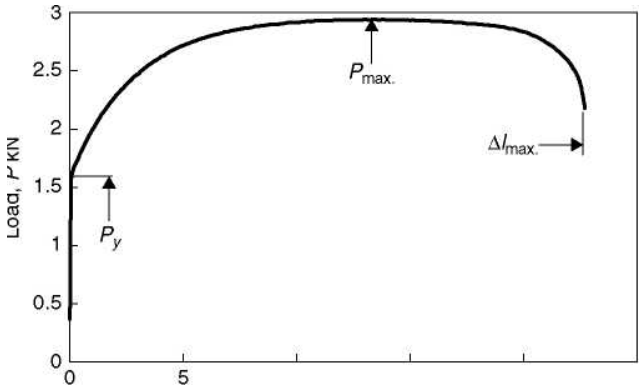

Fig 3.4 Load – Extension Diagram

Change in the Length(Δl) : Final Length – Initial Length

Δl : $l - l_0$

Δl : 62.80 – 50.00

Δl : 12.80 mm

Change in the width(Δw): Initial width at reduced section – Final Length at the reduced Section

Δw : $w_0 - w$

Δw : 12.50 – 9.28

Δw : 3.22mm

Engineering Stress

S : P / A_0

S : 7960 / 25.00

S : 318.40 N/mm^2

Engineering Strain

e : $(\Delta l / l_0) * 100\%$

e : 12.80 / 50.00 * 100%

e : 25.60%

Initial Yield Stress

S_y : P_y / A_0

S_y : 6250.00 / 25.00

S_y : 250.00 N/mm^2

Total Strain at 100% : 0.256

Yield Stress occurred at 3.5% of the Total Strain. Engineering Strain are as under:-

e_y : (0.04 / 0.256) / 100

e_y : 0.00156

Modulus of Elasticity

E : S_y / e_y

E : 250.00 / 0.00156

E : 1.603×10^5 N/mm^2

True Stress can be determined from the load – extension diagram during the rising part of the curve, between the yielding and maximum load, using the fact that plastic deformation in metals and alloys takes place without any appreciable change in volume. The volume of the gauge section is constant.

True Stress

σ : $P * l / (A_0 * l_0)$

σ : 7960 * 62.80 / (25.00 * 50.00)

σ : 399.91 N/mm^2

Strain increment

ε_{incr} : $\Delta l / l$

ε : 12.80 / 62.80

ε : 0.2038

True Strain

ε : $\ln (l / l_0)$

ε : ln (62.80 / 50.00)

ε : 0.2279

True Stress And strain at Yield Load :-

True Stress

σ_y : $P * l / (A_0 * l_0)$

σ_y : 6250 * 52.453 / (25.00 * 50.00)

σ_y : 262.265 N/mm^2

True Strain

ε_y : $\ln (l / l_0)$

ε_y : $\ln (52.453 / 50.00)$

ε_y : 0.0479

True Stress and Strain also be find from the Stress – Strain diagram. Calculation for the True Stress and True Strain are as under :-

True Stress

σ : $S * (1 + (e / 100))$

σ : $318.40 * (1 + (25.60 / 100))$

σ : 399.91 N/mm^2

True Strain ε : $\ln * (1 + (e / 100))$

ε : $\ln * (1 + (25.60 / 100))$

ε : 0.2279

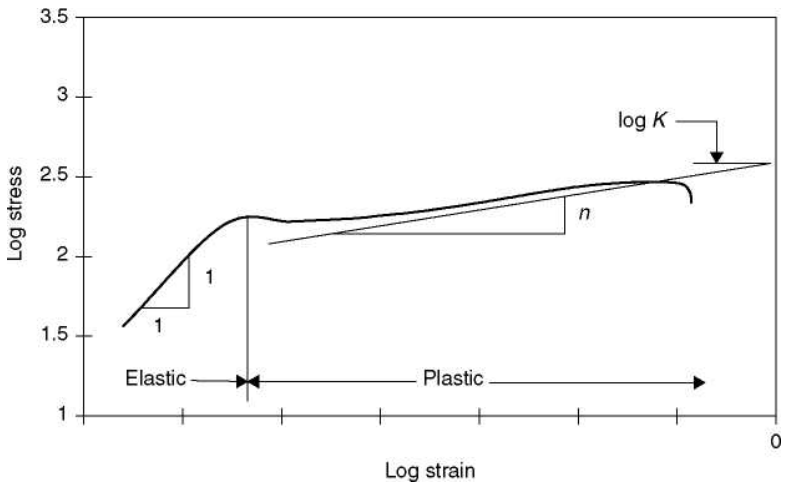

Fig 3.5 Stress Strain Curve

At Higher strain, the curve shown can be fitted by an equation of the form

σ : $K * \varepsilon^n$

Equation for n, Strain Hardening Exponent is as under

n : $(\log\sigma - \log\sigma_y) / (\log\varepsilon - \log\varepsilon_y)$

n : $(\log 399.91 - \log 262.265) / (\log 0.2279 - \log 0.0479)$

n : $(2.602 - 2.419) / ((-0.6423) - (-1.3197))$

n : $(0.183) / (0.6774)$

n : 0.270

Equation for K, Strength co-efficient is as under

K : $S * e^n / n^n$

Where, e :- 2.718

K : $318.40 * 2.718^{0.27} / 0.27^{0.27}$

K : $593.95\ N/mm^2$

Values of Stress according to Engineering Strain are as under:-

σ : $593.95 * 0.256^{0.27}$

σ : $411.13\ N/mm^2$

The fitted curve has a slop of n which is known as strain hardening index.

Same Calculation is done for another eight Specimen and got following results:

Specimen Type	σ	ε	σ_y	ε_y	n	σ_{eq}	ε_{eq}	ε_0	K
R001	430.008	0.322	272.508	0.066	0.289	430.008	0.322	0.0174	587.495
R002	421.294	0.252	294.014	0.067	0.271	421.294	0.252	0.0029	599.726
R451	389.312	0.234	288.760	0.067	0.239	389.312	0.234	0.0101	540.652
R452	396.511	0.236	265.090	0.049	0.255	396.511	0.236	0.0040	563.649
R453	408.960	0.245	283.331	0.057	0.253	408.960	0.245	0.0037	573.523
R901	386.677	0.233	262.509	0.039	0.216	386.677	0.233	0.0039	524.825
R902	405.720	0.231	285.962	0.057	0.251	405.720	0.231	0.0060	575.131
R903	395.012	0.230	257.475	0.029	0.208	395.012	0.230	0.0041	532.789

Table 3.2 Results from calculation

Calculation of Anisotropy:

Equation for finding the anisotropy

$$r = \varepsilon_w / \varepsilon_t$$

$$r = \frac{\ln \frac{w}{w_0}}{\ln \frac{w_0 l_0}{wl}}$$

Put the value in the above equation from table 1 which are getting form the tensile test.

For R003 Specimen,

$$r = \frac{\ln \frac{9.280}{12.50}}{\ln \frac{1.531}{2}}$$

$$r = 1.1147$$

Same way, calculate the value of r for eight specimen and the average of three Specimen which are cut in the same direction.

Specimen Type	Final Thickness	Final Width	Initial Width	Initial Thickness	r	Average of three reading
R001	1.633	8.700	12.5	2.00	1.7876	r_0=1.404563
R002	1.591	9.260	12.5	2.00	1.3114	
R003	1.531	9.280	12.5	2.00	1.1147	
R451	1.650	9.050	12.5	2.00	1.6789	r_{45}=1.692806
R452	1.631	8.560	12.5	2.00	1.8564	
R453	1.642	9.220	12.5	2.00	1.5431	
R901	1.642	9.510	12.5	2.00	1.3861	r_{90}=1.67114
R902	1.628	8.310	12.5	2.00	1.9839	
R903	1.652	9.130	12.5	2.00	1.6435	

Table 3.3 Results of Anisotropy

Calculation of Planar Anisotropy:

Equation for finding the normal plastic anisotropy,

$$R = \frac{r_0 + 2r_{45} + r_{90}}{4}$$

$$R = \frac{1.405 + (2*1.693) + 1.67114}{4}$$

$$R = 1.62$$

CHAPTER 4 THEORITICAL DETERMINATION OF FLD

There are so many models for Theoretical Determination of Forming limit Diagram. In this Report, Forming Limit Diagram Plotted using Combination of Swift and Hill model and NADDRG model.

4.1 Swift-Hill Model

The theoretical analysis is based on the plastic theory of Hill[9] taking orthotropic anisotropy into account, the equivalent stress σ_i and the equivalent Strain increment $d\varepsilon_i$ being defined as follows:

$$\sigma_i = \sqrt{\frac{3(1+r)}{2(2+r)}} \cdot \sqrt{\sigma_1^2 + \sigma_2^2 - \frac{2r}{1+r}\sigma_1\sigma_2}$$

$$d\varepsilon_i = \sqrt{\frac{2(1+r)(2+r)}{3(1+2r)}} \cdot \sqrt{d\varepsilon_1^2 + d\varepsilon_2^2 + \frac{2r}{1+r} d\varepsilon_1 d\varepsilon_2}$$

The associated flow rule in the principal axes of orthotropic anisotropy is expressed in the form:

$$\frac{d\varepsilon_1}{(1+r)\sigma_1 - r\sigma_2} = \frac{d\varepsilon_2}{(1+r)\sigma_2 - r\sigma_1} = \frac{-d\varepsilon_3}{\sigma_1 + \sigma_2} = \frac{d\varepsilon_i}{\frac{2(2+r)}{3}\sigma_i}$$

Where σ1, σ2, dε1 and dε2 are the major and minor principal stress and strain increment within the plane of a sheet, respectively, and dε3 is the thickness strain increment. The value *r*, which represents the anisotropic characteristics of the sheet, is the ratio of the width and thickness strain of a specimen deformed in uniaxial tension.

It has been proven that a good simulation of the forming limit strains can be given on the basis of the Swift diffuse instability theory and the Hill localized instability theory and here Swift's and Hill's theories are used to calculate the forming limit strains on the left and the right side, respectively, of the FLD.

Assuming that the stress–strain relationship of sheets can be expressed by Hollomon's equation:

$$\sigma_i = K\varepsilon_i^n \quad \varepsilon_i = \int d\varepsilon_i$$

Where *K* is a parameter of the material

n is the strain-hardening exponent.

According to Swift's and Hill's criterion combined with Eqs.19-20 , the formulae calculating the forming-limit strains can be written as follows, with

$$\alpha = \sigma_2 / \sigma_1$$

For $\varepsilon_2 < 0$:

$$\varepsilon_{j1} = \frac{1+(1-\alpha)r}{1+\alpha} n$$

$$\varepsilon_{j2} = \frac{\alpha-(1-\alpha)r}{1+\alpha} n$$

For $\varepsilon_2 > 0$:

$$\varepsilon_{f1} = \frac{[1+r(1-\alpha)].\left[1-\frac{2r}{1+r}\alpha+\alpha^2\right]}{(1+\alpha)(1+r)\left[1-\frac{1+4r+2r^2}{(1+r)^2}\alpha+\alpha^2\right]}.n$$

$$\varepsilon_{f2} = \frac{[(1+r)\alpha-r].\left[1-\frac{2r}{1+r}\alpha+\alpha^2\right]}{(1+\alpha)(1+r)\left[1-\frac{1+4r+2r^2}{(1+r)^2}\alpha+\alpha^2\right]}.n$$

After Using above Equation, with varying the value of stress ratio (α) we find the forming limit Diagram (FLD) as under:

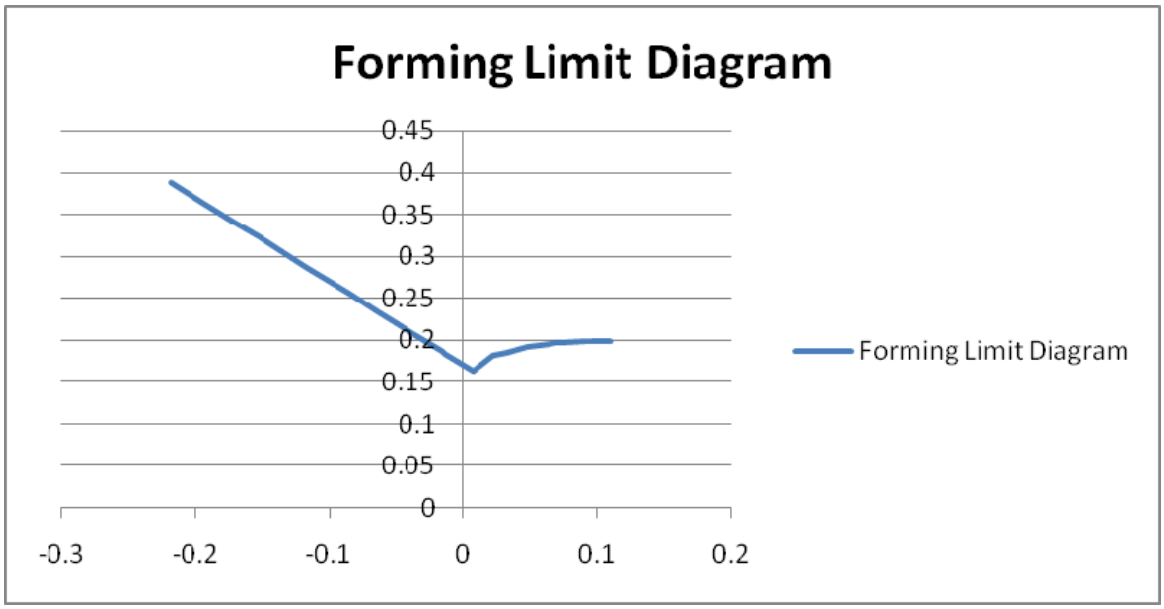

Figure 4.1 FLD based on Swift-Hill Model

4.2 NADDRG Model

For simplifying the experimental and theoretical determination of the FLD and utilizing the FLD more easily in the press workshop, the North American Deep Drawing Research Group (NADDRG) introduced an empirical equation for predicting the FLD in practice. This equation for calculating the forming-limit strain $e10$ in the plane-strain state in terms of engineering strain can be expressed as:

$$e_{10} = (23.3 + 360t)(n/0.21)$$

where $t_0 \leq 0.125$ is the sheet thickness in inches. According to this model, the FLD is composed of two lines through the point $e10$ in the plane-strain state. The slopes of the lines located respectively on the left- and right-side of the FLD are about 45° and 20°.

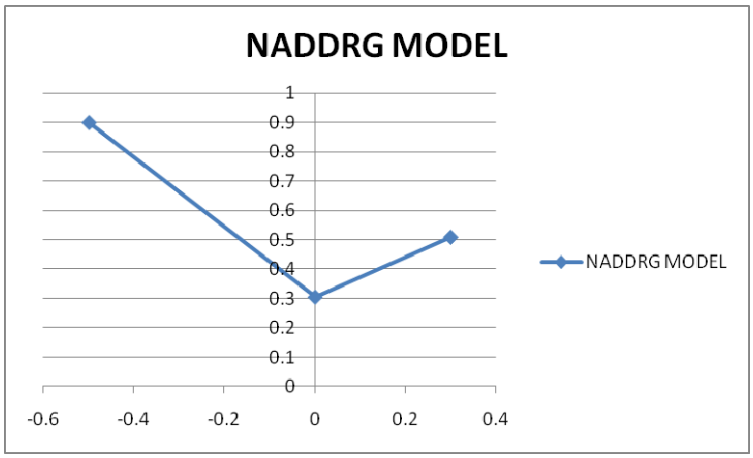

Figure 4.2 FLD based on NADDRG Model

CHAPTER-5 SIMULATION OF LIMITING DOME HEIGHT (LDH) TEST

5.1 Modeling of LDH Test

Fig 5.1 shows tooling geometry prepared for Experiment on the basis of guideline given in the ASTM E2218-02 Standard. Modeling of Limiting Dome Height test was done in the PRO-E Wildfire 3.0

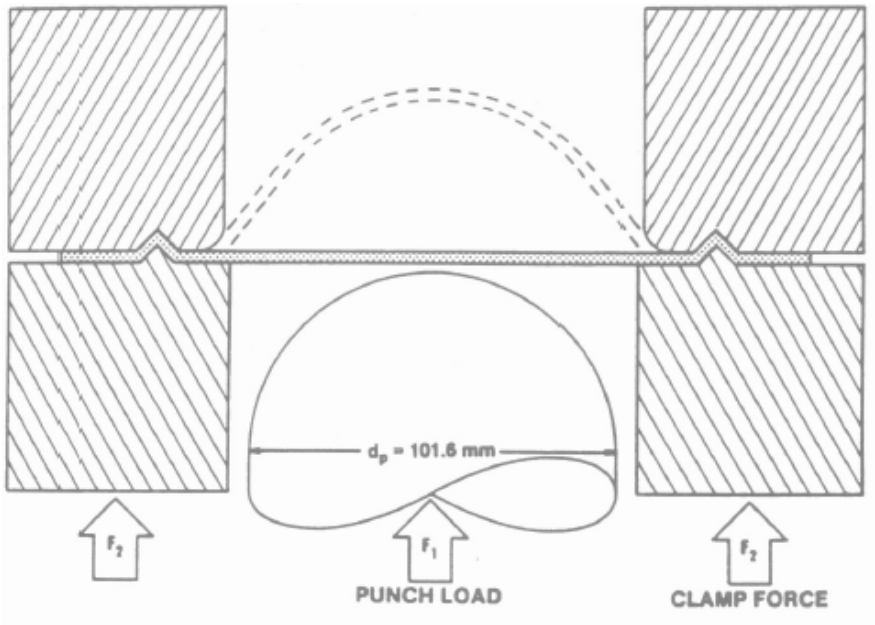

Fig 5.1 Geometry of LDH Test

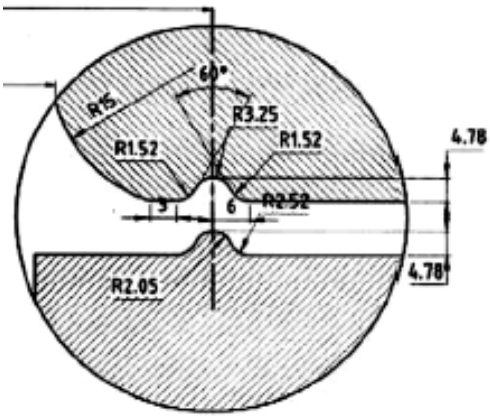

Fig 5.2 Geometry of Draw bead

The Triangular drawbead was modeled on the die surface with height of 4.78 mm and width of 6 mm and was positioned at a distance of 132.68 mm from the center of the die block. Accuracy of

the Experimental Result is large extent dependent on the drawbead because if the drawbead position or dimensions are not appropriate then there is a chance of drawing rather than stretching.

5.1.1 Procedure of Modeling:-

- Die, Binder and Forming Punch are modeled in Part modeling mode.

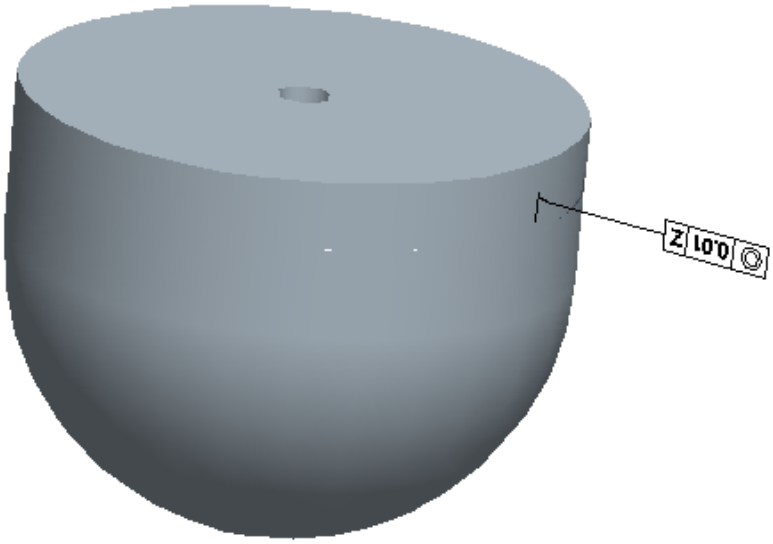

Fig 5.3 Forming Punch

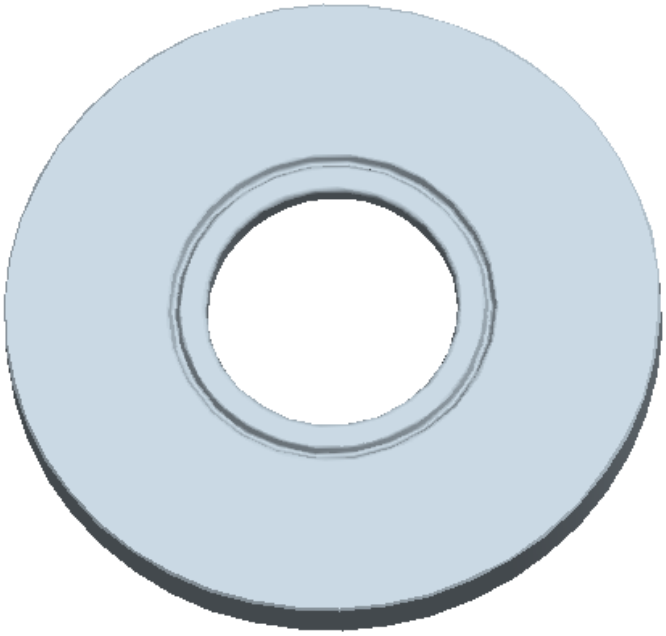

Fig 5.4 Binder

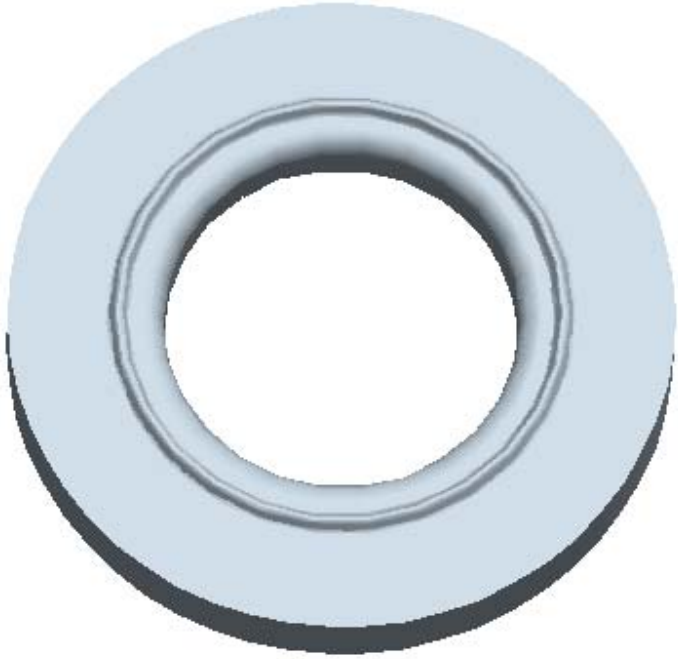

Fig 5.5 Die

- Assemble the geometry in the Assembly mode.

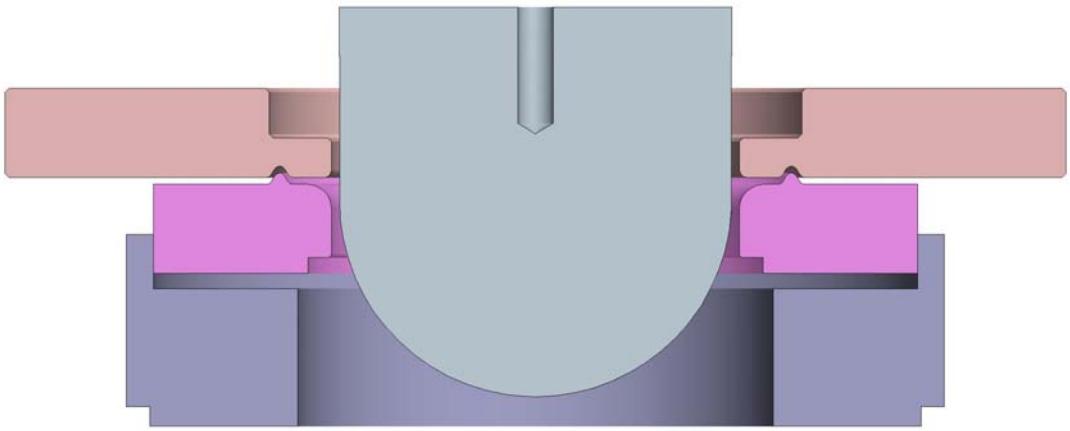

Fig 5.6 Assembly in PRO-E

- Prepare the Manufacturing drawing of all parts and also prepare assembly drawing for reference to the operator while loading the tool on the press.

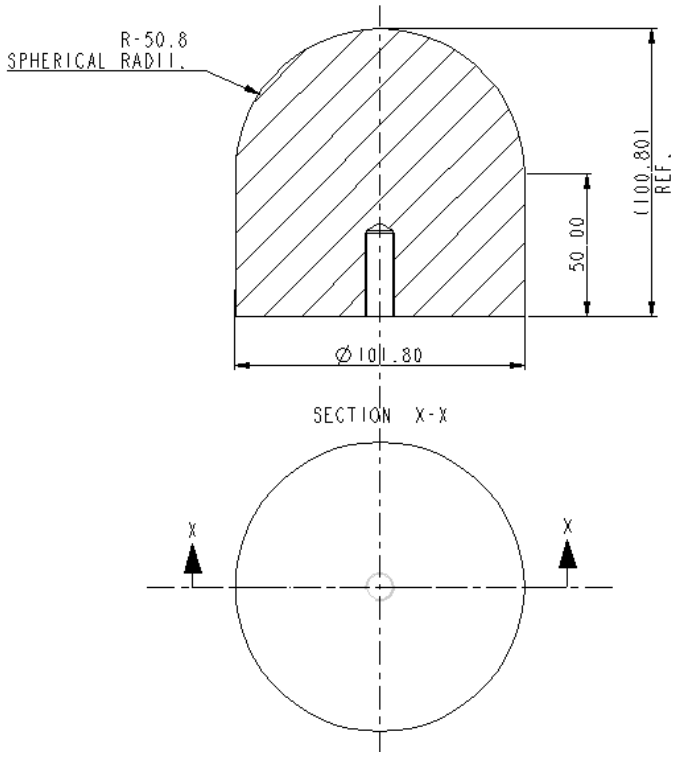

Fig 5.7 Manufacturing Drawing of Forming Punch

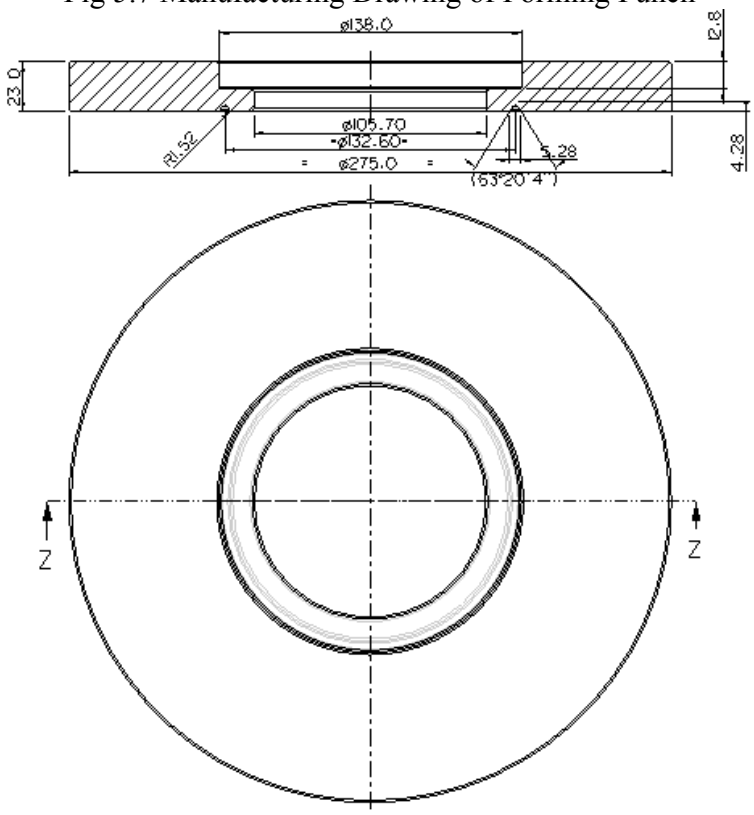

Fig 5.8 Manufacturing Drawing of Binder

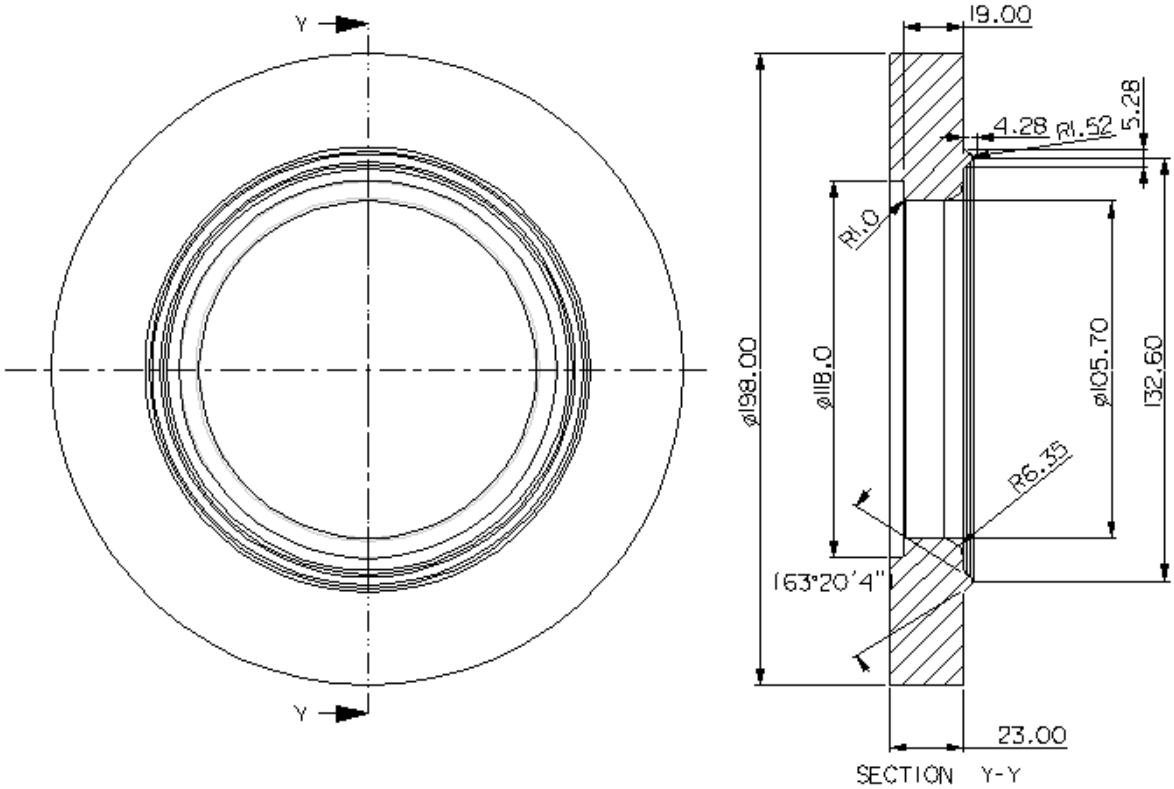

Fig 5.9 Manufacturing Drawing of Die

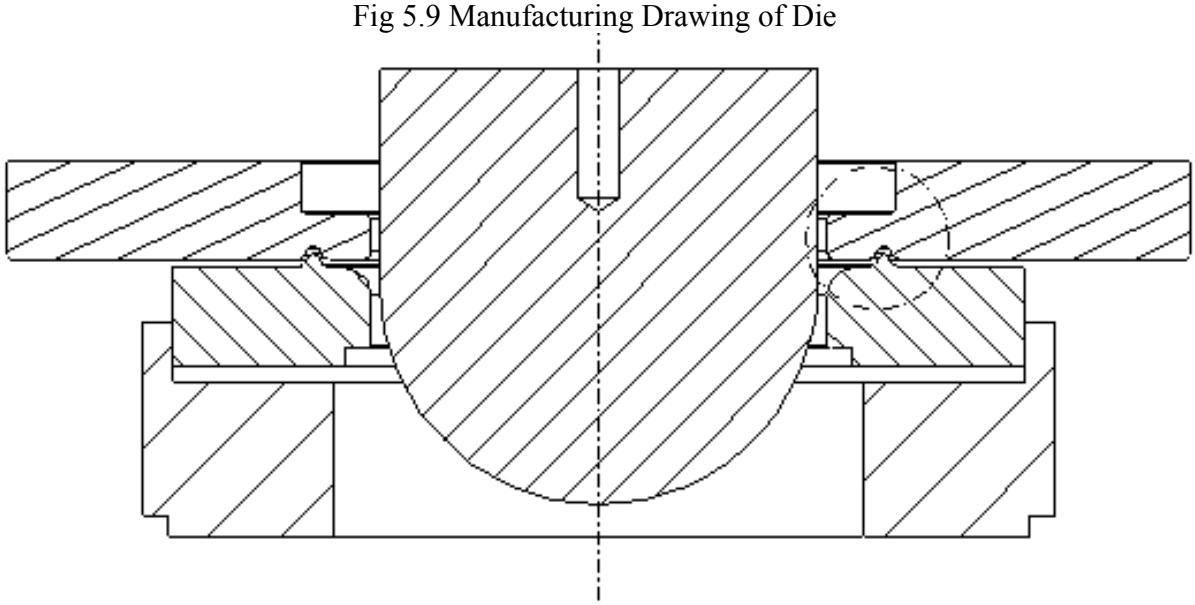

Fig 5.10 Assembly of LDH Test

5.2 Analysis of LDH Test

5.2.1 Analysis Procedure

Fig. 5.10 shows the general work flow diagram adapted to model and solve problem by FEA. The punch and die set assembly along with the specimen was modeled in Pro-E Wildfire 3.0 and exported as *.IGES in Hyperform.

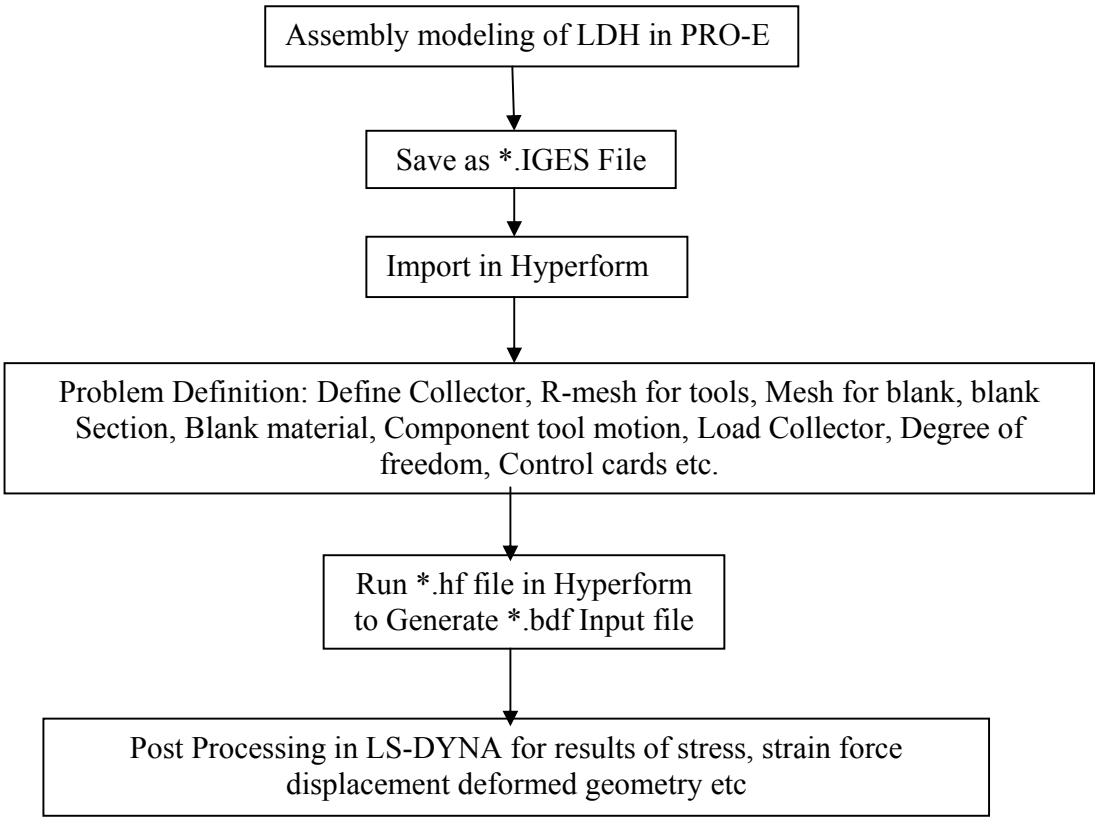

Fig 5.11 Workflow Diagram

Hyperform has a three module of operation.

Module 1- Pre-Processing (Meshing,Appling boundry condition etc)

Hyperform is used as simulation tool for the numerical analysis. Numerical model for punch, die, blank, and blankholder are shown in Figure 5.11.The Punch and die are modeled using shell elements with surface mesh option. They have assigned RIGID_MATERIAL_MODEL.The blank is assigned TRANSVERSELY_ANISOTROPY_ELASTIC_PLASTIC_MODEL.

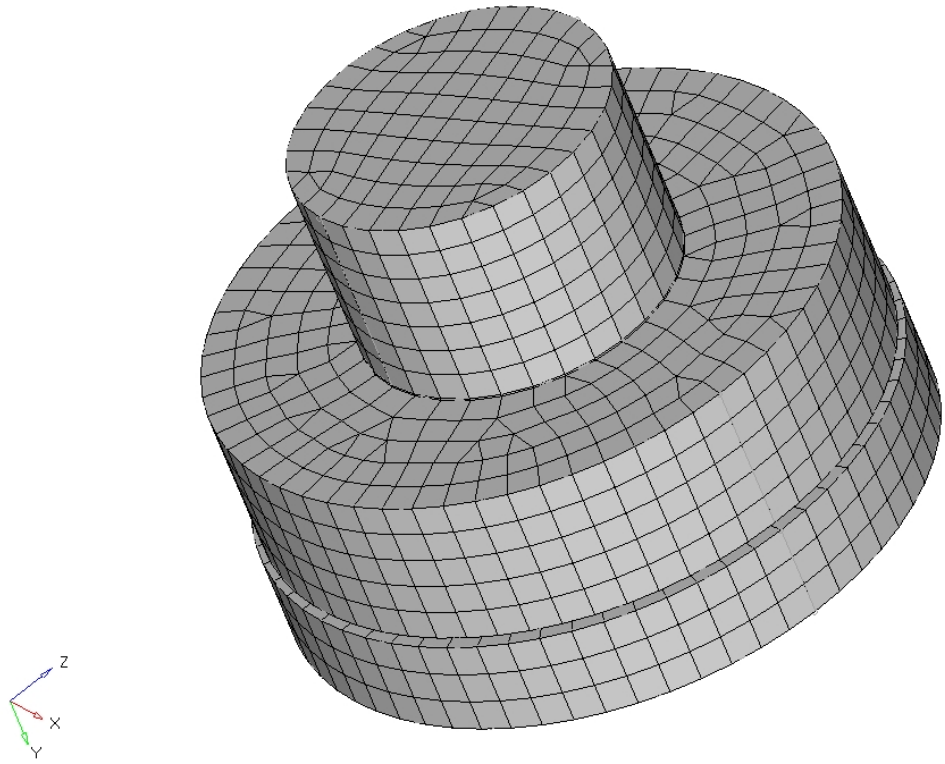

Fig 5.12 Meshing Geometry of LDH Test

Input Condition for Simulation:-

Blank material ;- AISI 1008

Yield Strength :- 250 N/mm^2

Ultimate Strength:-318 N/mm^2

Strain hardening Exponent:-0.270

Pre-Strain:-0.018

Strength Coefficient:-593.95

R_0:-1.405

R_{45}:-1.693

R_{90}:-1.67114

Press Speed - 45 SPM

Punch Stroke :- 45mm

Binder force:-35KN

Module 2:- Solver

After giving all input conditions to hyperform, Run analysis which create the .bdf file which is the input file for “LS-DYNA”Solver. This input file give to LS-DYNA which solve the problem and generate d3plot file which is a post processing file.

Module 3:- Post Processing

Load d3plot file on the load result panel of hyperform which open the hyperview for viewing the results. Choose new study on the panel of FLD Creator and choose the component as blank which create FLD as shown below.

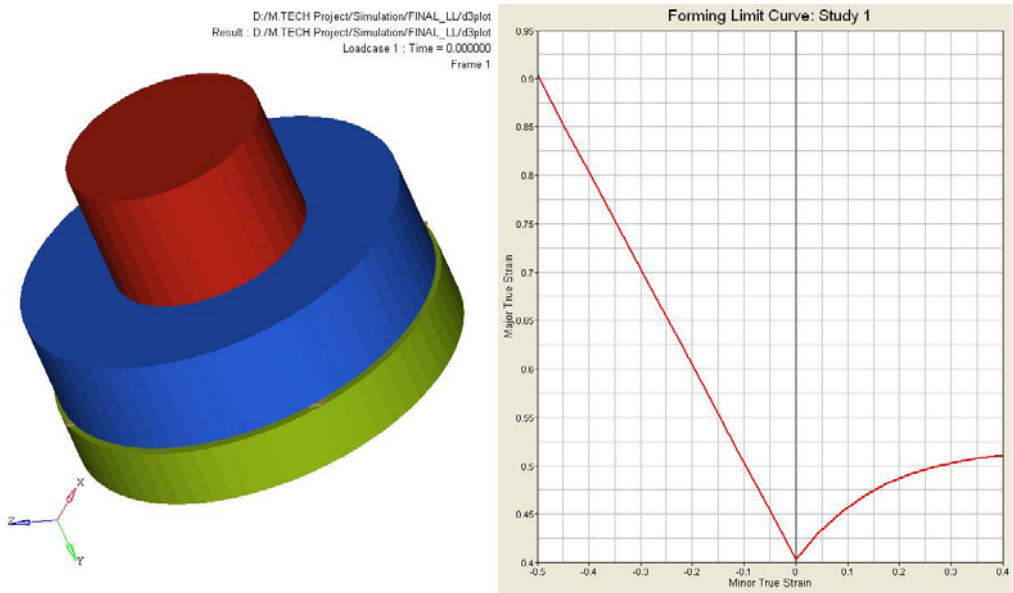

Fig 5.13 FLD by Hyperform

CHAPTER-6 EXPERIMENTAL DETERMINATION OF FLD BY LIMITING DOME HEIGHT TEST, ERICHSON TEST AND TENSILE TEST

6.1 Limiting Dome Height Test:-

Figure 5.1 shows the tooling and a typical sheet specimen after fracture The height of the dome at maximum load (near failure) which combines the effect of forming limit with requisite strain distribution for that strain rate is employed as a measure of strechability. The LDH test uses a 101.6 mm ball to stretch to fracture a circular sheet The dia. of the specimen is varied to provide a minimum dome height known as a limiting dome height In order to determine the LDH minimum strip specimen of different dia. are used this test assesses the formability performance of a material in or near plane strain stretching condition which is the most detrimental condition in stamping. This test is very sensitive to punch conditioning and punch temperature effects. Although the test fails to distinguish among different contributions to the materials formability such as base metal, cooling and lubricant properties. It is capable of detecting overall changes in formability.

For Carrying out Limiting Dome Height Test, Binder, Die, Forming Punch, etc. are manufactured as per Guideline given in the ASTM E2218-02 Standard. table 6.1 shows bill of material for Limiting Dome Height test tool.

Sr. No	PART NAME	MATERIAL	QTY.
1	Binder	M.S	1
2	Die	D2	1
3	Forming Punch	HcHcr	1
4	Binder Housing	EN-24	1
5	Die Housing	C45	1

Table 6.1 Bill of Material

6.1.1 Press Specification which is used for Experiment Work.

Manufacturer:- Chinfong, China

Model :- OCP-110

Capacity :- 110 tons

Slide Area :- 650 * 520 mm

Bolster Area :- 1150 * 680 mm

Main Motor :- 7.5 Kw

6.1.2 Blank Specification Used for Experimental Work:-

Blank Material: - AISI 1008

Manufacturer of Coil:-Ahmedabad Steel Pvt. Ltd

Parent Coil Manufacturer: - Essar Steel

Blank thickness:- 2 mm

Blank Dia.:- 202mm

Blank Qty:- 4 piece of Each Dia.

6.1.3 Chemical Analysis of Blank

Chemical Analysis is done by Spectrometer. A spectrometer is an optical instrument used to measure properties of light over a specific portion of the electromagnetic spectrum, typically used in spectroscopic analysis to identify materials. The variable measured is most often the light's intensity but could also, for instance, be the polarization state. By measuring wavelength and intensities chemical composition of the material is determined.Total four Specimens are tested for different Grain Direction.

Specification of Spectrometer:-

Manufacturer: - Arun Technology,

Model Name:-Metal Scan Desktop Metals Analyzer-2500

Results from Spectrometer:-

Sr No.	Fe	C	Si	P	S	Mn	Ni	Mo	Cu	Al	V
0	99.57	0.0318	0.11	0.0381	0.0203	0.146	0.0368	0.187	<0.005	0.0083	<0.003
45	99.43	0.0375	0.203	0.0324	0.0221	0.158	0.044	0.0193	<0.005	0.0338	<0.003
90	99.55	0.0371	0.0996	0.0353	0.204	0.15	0.0347	0.0203	<0.005	0.0337	<0.003
90	99.52	0.0154	0.172	0.0391	0.0215	0.157	< 0.03	0.0177	<0.005	<0.008	<0.003

Table 6.2 Composition of AISI 1008

6.1.4 Circle Grid Marking:-

Grid marking is done by laser Source. Here the Circle of 2.5mm dia. is etched on the blank as shown in figure. In this Experimental Work, total 16 Specimen (16 trial) is used for determination of Forming Limit Diagram.

Fig 6.1 Grid marked on the LDH Test blank

6.1.5 Experimental Set up:-

Fig 6.2 Shows Set up which is used for determination of FLD. Limiting Dome Height tests are conducted using the standards LDH test geometry which makes use of 101.6 mm diameter hemispherical punch. Sample diameter varied. The sheet samples are laser marked with a circle of 2.5mm diameter. Sample are clamped with binder force of 35 KN to prevent draw-in and tested to failure with the help of four gas spring. The major and minor axes of the deformed circles are measured with the help of a travelling microscope (tool makers microscope), to calculate strains. Ellipses lying in the cracked or the necked region are considered failed and the rest are considered to be safe.

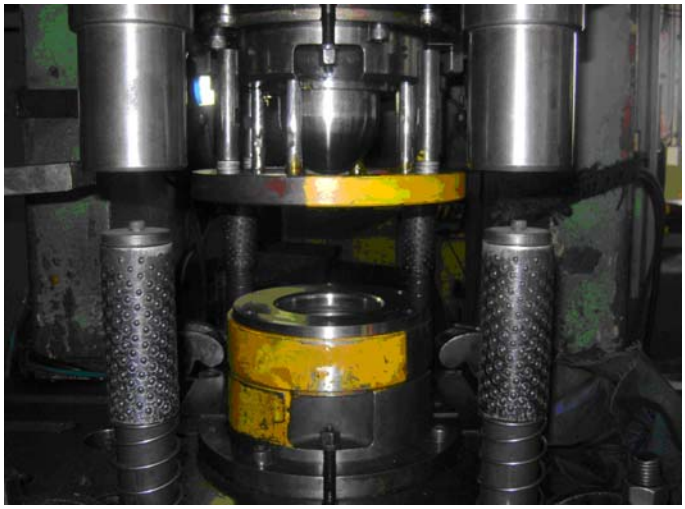

Fig 6.2 Experimental Set up for LDH Test

6.1.6 Grid Measurement System:-

Deformed Grid is measured with the help of Tool Makers Microscope (Travelling Microscope).

Fig 6.3 Tool makers Microscope

Specification of Tool Makers Microscope:-

Manufacturer:- Mitutoyo, Japan

Model No. :- TM-500

Calibration Date:-2/2/2008

Calibration Due:-2/2/2010

Calibrated by:- Mitutoyo South Asia Pvt. Ltd

6.1.7 Experimental Procedure for Determination of FLD:-

- 16 Specimen is Cut from the Strip by Circle Cutting tool
- Circle Grid Marking is done by Laser Source.
- Grid marked blanked put on the press.
- Take the trail by Press with Speed setting of 45 SPM.
- Remove the Specimen from the Press.
- Specimen is taken to the Tool Makers Microscope for deformed Grid Measurement.
- Take 10 points from 0, 45, 90 Direction.
- Plot Forming Limit Diagram Using the Eq (a) and (b).

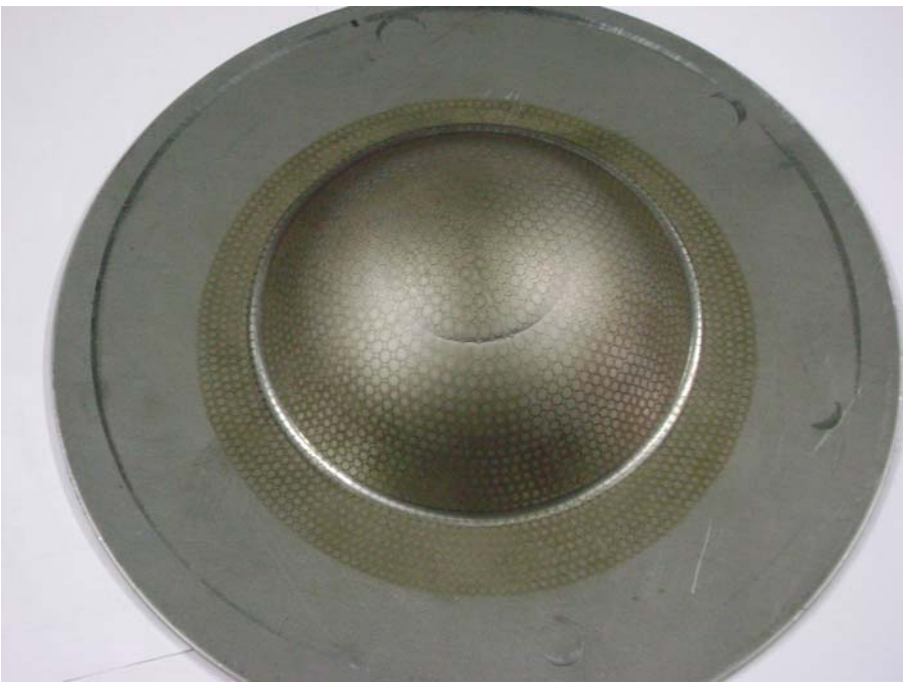

Fig 6.4 Deformed Specimen of LDH Test

6.1.8 Results from LDH Test

In this Experimental Work, Total 30 Grids are measured all around the Specimen for determination of FLD.

10 Grids – Rolling Direction

10 Grids – Angular Direction

10 Grids - Transverse Direction

Forming Limit Diagram for Blank Dia – 200 mm and Blank Thickness – 2.00 mm is shown.

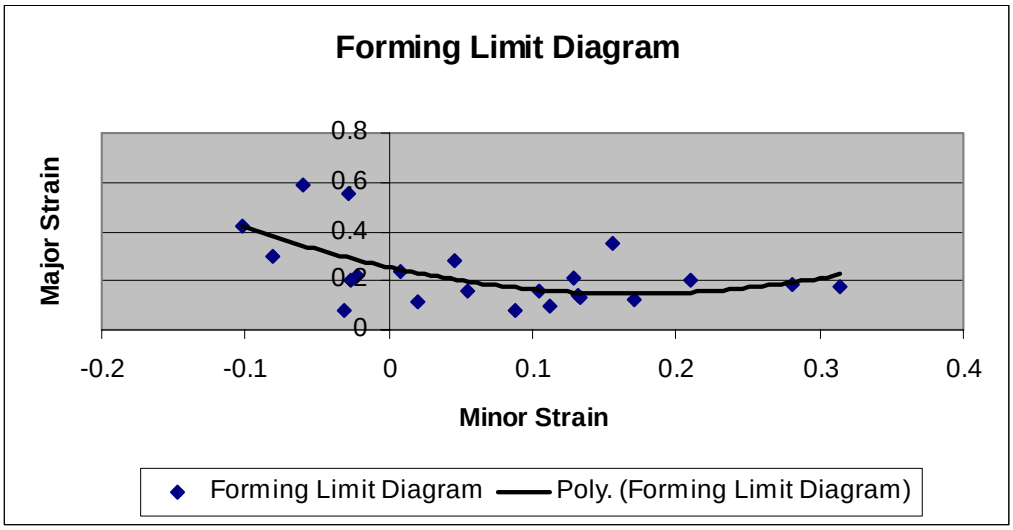

Fig 6.5 Forming Limit Diagram based on LDH Test

6.2 Erichsen Test:-

The Erichsen were the first tests developed to estimate sheet metal formability under stretching conditions. In test, the sheet is clamped between two polished fiat plates with a hole of diameter equal to 25.4 mm and a ball of diameter, d, is pressed into the sheet metal until failure occurs. The height of the cup, h at failure is used as the formability index (for Erichsen test d is equal to 20 mm). The larger this height, h, the greater is the sheet metals ability to resist necking instability during stamping.

Fig 6.6 Shows Experimental Set up Which is used for Erichson Testing. This Set up is manufactured by FUEL INST & ENG PVT LTD.

Fig .6.6 Experimental Set Up for Erichson test

6.2.1 Specification of Erichson Testing Machine:-

Model No.		ET-20
Technical Data	Unit	-
Width of sample	mm	70-90
Thickness of sample	mm	0.1-2
Least count	mm	0.01
Overall Dimensions	mm	450x500x500
Net weight (approx)	kg	20

6.2.2 Circle Grid Marking:-

Grid marking is done by laser Source. Here the Circle of 2.5mm dia. is etched on the blank as shown in figure. In this Experimental Work, total 24 Specimen (24 trial) is used for determination of Forming Limit Diagram.

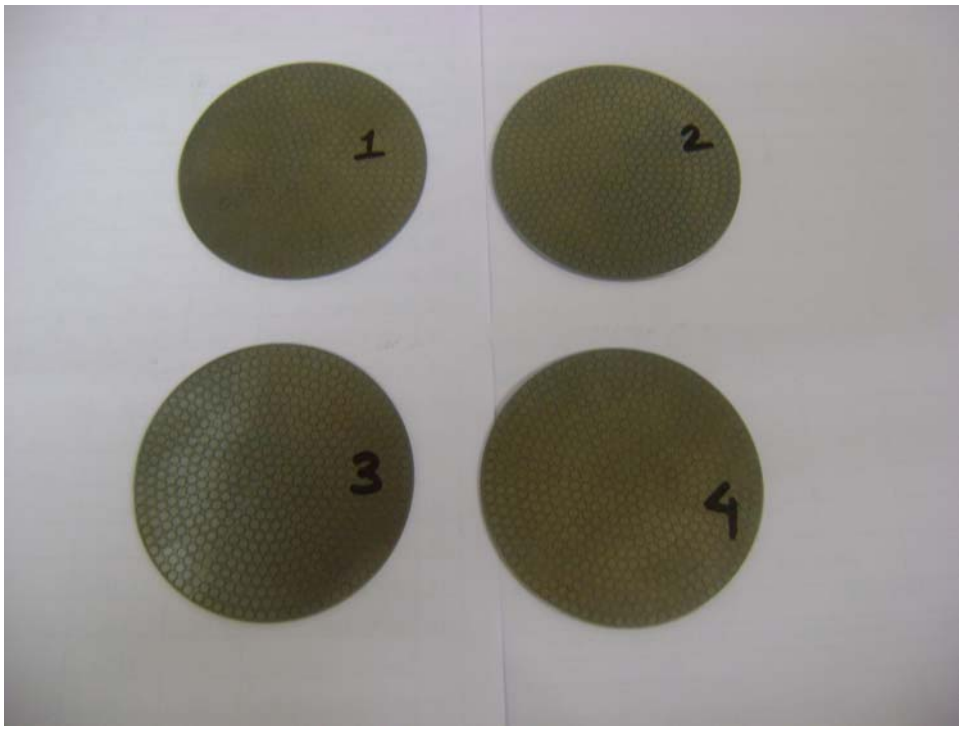

Fig 6.7 Grid Marked Blank of Erichson Test

6.2.3 Blank Specification which is Used for Experimental Work:-

Blank Material: - AISI 1008

Manufacturer of Coil:-Ahmedabad Steel Pvt. Ltd

Parent Coil Manufacturer: - Essar Steel

Blank Dimensions are shown in below table:-

Blank Dia	Thickness
105.5	1.5
66	1
104	1.2
75	1.25
100	2

Table 6.3 Blank Dimension of Erichsen Test

6.2.4 Experimental Procedure:-

- 24 Specimen is Cut from the Strip by Circle Cutting tool

- Circle Grid Marking is done by Laser Source.
- Grid marked blanked put on the Erichson Testing Machine.
- Fix the Blank between Binder and Die by application of manual load on the fixing wheel.
- Take the trail by appling manual load on the Load wheel of machine. When the load is applied punch move outwards and stretch material.
- See in the mirror which is fitted in the front of the punch while appling load.
- Stop the test when the Crack is generated.1
- Remove the Specimen from the Erichson Testing Machine.
- Specimen is taken to the Tool Makers Microscope for deformed Grid Measurement.
- Take 5 points from 0, 45, 90 Direction.
- Plot Forming Limit Diagram Using the Eq. (a) and (b).

Fig 6.8 Deformed Specimen of Erichson Test

6.2.5 Experimental FLD by Erichson Test:-

In this Experimental Work, Total 15 Grid are measured all around the Specimen.

5 Grids – Rolling Direction

5 Grids – Angular Direction

5 Grids - Transverse Direction

Here the Forming Limit Diagram for Blank Dia – 100 mm and Blank Thickness – 2.00 mm is shown.

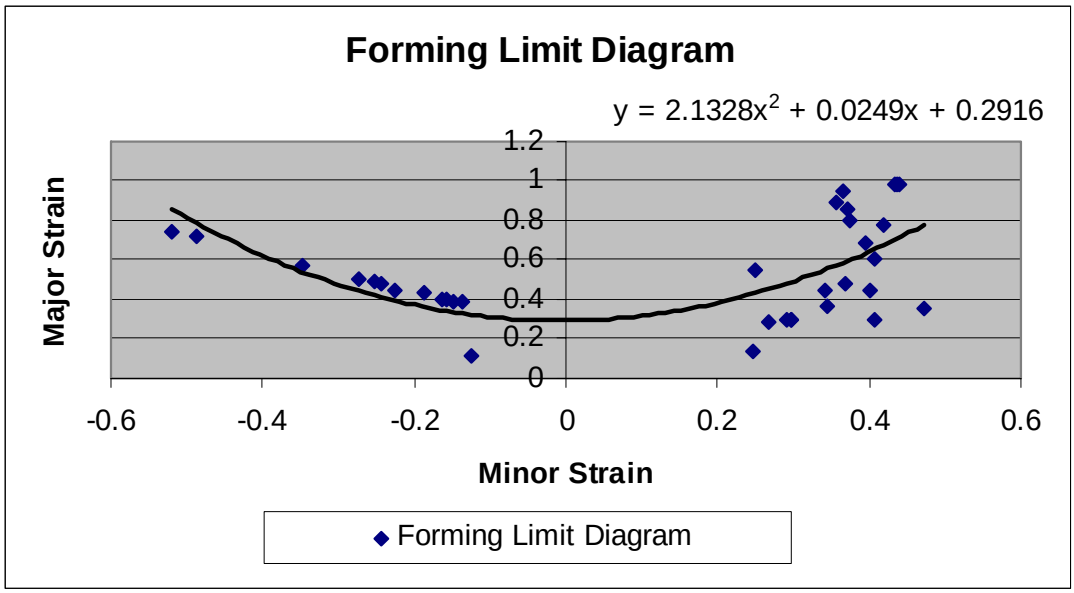

Fig 6.9 Forming Limit Diagram by Erichson Test

6.3 Tensile Test:-

FLD by tensile test enables fast and easy determination of forming limit and shows less scatter in results. The test procedure applied only the negative side of the FLD because this is the case of Uniaxial Tension.

6.3.1 Specimen Used for Experimental Work:-

Specimen Material: - AISI 1008

Manufacturer of Coil:-Ahmedabad Steel Pvt. Ltd

Parent Coil Manufacturer: - Essar Steel

Specimen thickness:- 2 mm

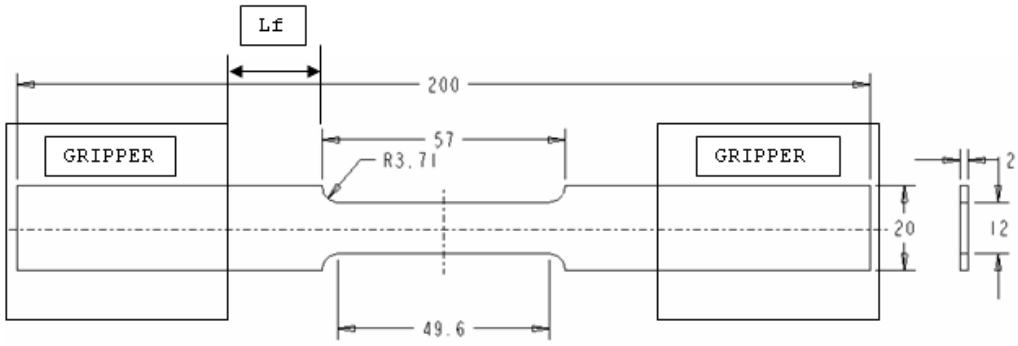

Fig 6.10 Tensile Test Specimen

Fig 6.10 shows the geometry of Test Specimen Which is as per ASTM E8 Standard.

6.3.2 Circle Grid Marking:-

Grid marking is done by laser Source. Circle of 2.5mm dia. is etched on the Tensile Test Specimen for finding the strain.

6.3.3 Experimental Procedure:-

Tensile testing machine is built up with a load frame of a solid T-slot table, columns and a hydraulically maneuverable crosshead. Control and data acquisition is performed by computer boards and specially designed programs. Test is performed on Universal Tensile Testing machine which is manufactured by FIE. To be able to clamp the specimen in the desirable manner, special attention was put on the rectangular jaw rather than circular jaw, and specially their surface towards the specimen.

Fig 6.11 Experimental Set up for Tensile Test

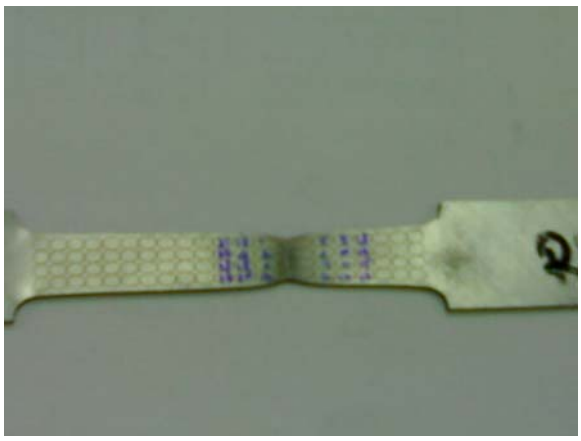

Fig 6.12 Deformed Specimen of Tensile Test

6.3.4 Forming Limit Diagram by Tensile Test:-

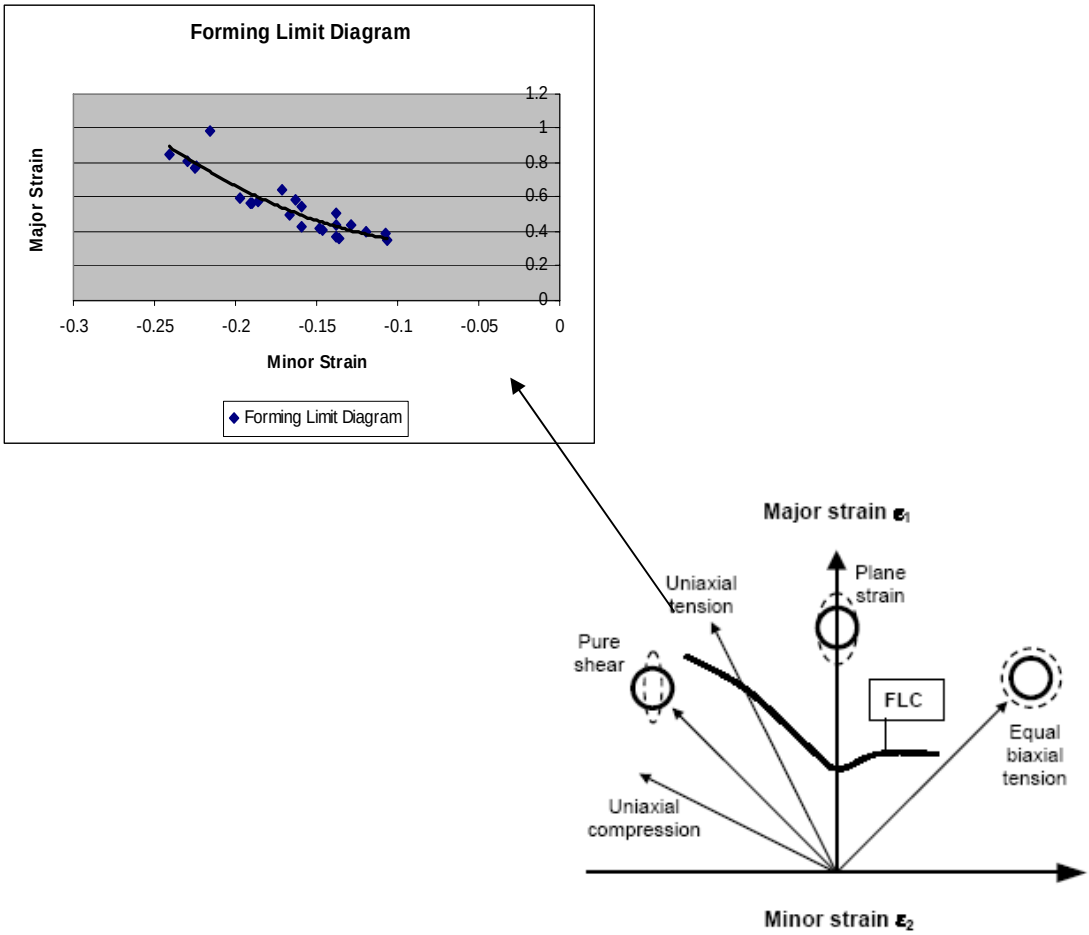

Fig 6.13-Forming Limit Diagram by Tensile Test

- A test procedure for determining the forming limit in plane Diagram by Tensile Test for sheet metal was developed. The results show small scatter as compared to the conventional methods and it can be carried out in a tensile testing machine. It does not require any forming tools or press.
- The grip arrangements are essential in order to get successful tests. With insufficient clamping of the specimen, localization and fracture will not occur at the desired middle region of the specimen where plane strain conditions apply.
- The specimen free length (L_f) has a large influence on the results. The specimen free length should be as small as possible in order to get a condition as close to plane strain as possible in the middle region of the specimen.

- A test procedure for determining the complete left-hand side of the FLC by tensile tests was outlined. By changing the geometry of the specimen, different strain conditions are achieved. The right-hand side of the FLC cannot be determined by this procedure.

CHAPTER-7 FLD BY DIFFERENT METHODS

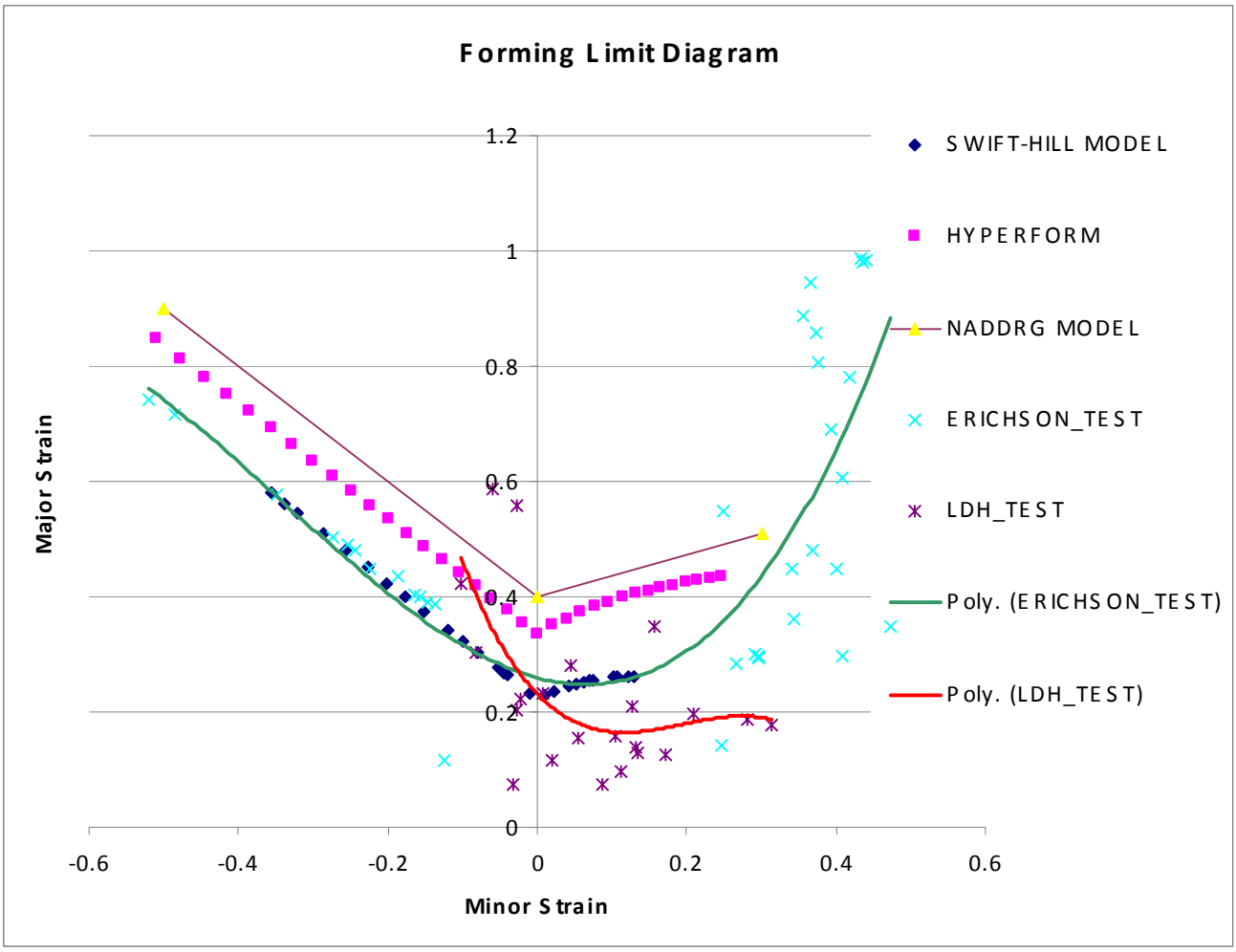

Figure 7.1 shows Comparison of theoretical FLDs, Experimental FLDs and FE FLD.

- The Hyperform results show FLC at higher level than combined swift-hill model and lower than NADDRG Model. Results of Erichsen test(Experimental) closely matches with Swift-Hill Models (theoretical model).

CHAPTER-8 CONCLUSIONS & FUTURE SCOPE

CONCLUSIONS

An analysis of the deformation behavior of AISI 1008 Steel through usage of uniaxial tensile Test, Limiting Dome Height Test and Erichson Test was undertaken in the present study. Correlation of the formability parameters and the forming limit diagrams was analyzed.

The following conclusions were determined on the basis of this work.

- If new forming Component is to be designed based on FE FLD then suitable factor of safety should be taken in the range of 5-10 percent reduction.
- The FLD_0 value is met by the empirical NADDRG model and the FE simulation with sufficient accuracy. The Swift-hill model delivers too small FLD_0 Value.
- The Hyperform results show FLC at higher level than combined swift-hill model and lower than NADDRG Model. This shows NADDRG model can be used initially to begin with design of new forming Component.
- FLD from analytical (Swift-Hill methods) methods and experimental methods matches closely.
- Finite Element Results Shows that FEA is a good and reliable tool with good accuracy which can replace time consuming and costly experimental work.
- The accuracy of the theoretical and FEA simulation are large extent dependent on the material properties provided as an input.

Future Scope

- The forming limit diagram is affected by the thickness, the yield and tensile strength, strain hardening exponent and plastic anisotropy So Design of experiments may be carried out to arrive at effect of one parameter on the FLD keeping other parameter constant and such procedure can be repeated for all the parameters and then combined effect on FLD can be studied.

REFERENCES

[1]H.W.Swift, Plastic instability Under Plane Stress, *J. Mechanics and Physics of Solids*,1952,vol.1,pp 1 to 18.

[2]R.Hill,On discontinuous plastic states with special reference to localized necking in thin Sheets, *J.mechanics and physics of solids*, vol 1 pp 19 to 30.

[3]Z.Marciniak,J.L.Ducan,S.J.Hu,Mechanics Of Sheet Metal Forming,page61-79.

[4]Z.Marciniak and K.Kuczynski,Limit Strain in the processes of strech-forming Sheet metal,*Int.J.Mech.Sci*,1967,vol 9,pp 609-620.

[5]K.Narasimhan,M.P.Miles,R.H.Wagoner,A better Sheet-Formability Test, *J.Mater . process.Technol 50*(1995) 385-394.

[6] Henry E. Theis, Handbook of Metal Forming Processes , page3-61.

[7] ASTM E2218-02 Standard test method for determining forming limit curves.

[8] ASTM E8-04 Standard Test Methods for Tension Testing of Metallic Materials.

[9] R.Hill, The mathematical theory of plasticity,clarendon Press. Oxford

[10] J.Z.Gronostajski and Z.Zimniak, Theoretical Simulation of Sheet behaviour in Forming processes, *Journal of materials Processing Technology*,31(1992)57-63.

[11]V.Talyan,R.H.wagonar and J.K.lee,Formability of Stainless Steel, *Metallurgical and Materials Transactions A* ,Volume 29A,August 1998-2161.

[12] www.cpforming.org visited on 27th September,2008.

[13] www.ercnsm.org visited on 27th September,2008.

[14] V.Buakaew, S.Sodamuk, S.Sirivedin and S.Jirathearanat, Formability Prediction of Automotive Parts Using Forming Limit Diagrams, *J.Solid Mechanics and Materials Engineering* ,vol.1,pp 691-698

[15]Stefan Holmberg, Bertil Enquist ,Per Thilderkvist, Evaluation of sheet metal formability by Tensile tests, *J.Materials Processing Technology* 145(2004) 72-83

[16] Amit Mukund Joshi,Strain Studies in Sheet Metal Stampings.

[17] David A. Smith, Fundamental of Press Working, Society of Manufacturing Engineers,1994.page no.135-140.